LIFT COEFFICIENTS OF SPHERES MOVING IN CIRCULAR TUBES

by

Richard Allan Hendrickson

A Thesis Submitted to the
Graduate Faculty in Partial Fulfillment of
The Requirements for the Degree of
MASTER OF SCIENCE

Major Subject: Nuclear Engineering

Approved:

Signatures have been redacted for privacy

Iowa State University
Of Science and Technology
Ames, Iowa

1962

TABLE OF CONTENTS

INTRODUCTION

The fact that flowing fluids have the capacity to suspend and transport solid particles is of great importance in many industries. Coal, grain, sand, and cement represent a few materials that may be transported by moving streams of air or water in pipe lines. The operation of the homogeneous nuclear reactor is dependent upon the suspension and transportation of fissionable fuel to and from the reactor core. Chemical processing of nuclear fuels also involves the movement of fissionable material in suspension. In the latter, great care is exercised to prevent unwanted holdup of solids to avoid creating a critical assembly of fuel.

Although a large amount of empirical information is available to aid the designer of slurry systems, many problems concerning the behavior of flowing suspensions and the incipient motion of a bed of particles are unsolved. Answers to the questions, why do solids remain in suspension, and why and when do particles resting on the bottom of a pipe move, are basic to the understanding of the properties of slurries. It follows, then, that the evaluation of the forces acting on the individual particle is of basic importance.

The component of the resultant fluid force acting parallel to the direction of particle motion is called drag, and the component normal to the path is termed lift. For over

one hundred years, studies of the behavior of a particle moving in a fluid medium have been primarily concerned with the resisting force, or drag, and little attention has been given to the lift component.

The objective of this investigation was to examine the variables that influence the lift coefficient of a single spherical particle moving in a still fluid contained in a circular tube. The lift coefficient was conventionally defined as

$$C_L = \frac{L}{\rho_f A \frac{V^2}{2}} \qquad (1)$$

where L = lift

ρ_f = fluid density

A = cross sectional area of the sphere

V = velocity of the sphere

In this investigation, lift was defined as the force normal to the pipe wall. It was equal to the normal component of the weight of the particle in the fluid.

A prediction equation was developed that relates the lift coefficient to the examined variables.

REVIEW OF THE LITERATURE

A generalized analytical determination of the fluid forces acting on a sphere as it moves through a still, viscous fluid is improbable. Jensen (1, p. 349) ably sets the problem in perspective when he states that

> . . . The Navier-Stokes equation being non-linear has so far proved insoluble for the problem of axi-symmetric flow around spheres, except by methods which first linearize the equations by approximations.

These approximations usually severely limit the solutions.

The classical mathematical solution for the drag acting on a slowly moving sphere in an infinite fluid was performed by Stokes (2) in 1851. The equation is given as

$$F = 3 \pi \mu v d$$

where F is the drag, μ is the fluid viscosity, v is the sphere velocity and d is the sphere diameter. This expression is limited to Reynolds numbers of less than one.

Ladenburg (3) examined the effect of boundaries on the fall-velocity of a sphere in a cylindrical pipe in 1907. He found that the influence of the tube wall on the particle motion was detectable in a tube which had a diameter one hundred times that of the sphere. These tests were performed at Reynolds numbers less than one.

McNown *et al.* (4) experimentally determined the influ-

ence of a cylindrical boundary on the drag of spheres for Reynolds numbers from zero to 1,000 and for diameter ratios from zero to one. Their objective was the definition of the function

$$K = f(\frac{d}{D}, N)$$

where $\frac{d}{D}$ is the sphere to tube diameter ratio, N is the Reynolds number and K is a variable coefficient used to modify Stoke's equation for the effect of the boundary. The modified equation is given by

$$F = K(3 \pi \mu v d)$$

The coefficient, K, is also related to the drag coefficient C_D by the expression

$$K = \frac{C_D N}{24}$$

where C_D is defined conventionally by the relationship

$$C_D = \frac{F}{\rho_f A \frac{V^2}{2}}$$

where ρ_f is the fluid density, and A is the cross-sectional area of the sphere. The experimental results are presented in graphical plots showing the variation of K with $\frac{d}{D}$. The authors state that a Reynolds number based on the sphere

dimension may not be sufficient for comparison due to the change in boundary geometry with diameter ratio.

Young (5) determined the lift acting on a spherical particle resting on the wall of an inclined tube in which a fluid was flowing. Experimental data are presented to show the variation in lift and drag coefficients with diameter ratio and Reynolds number. An equation is presented to predict the lift coefficient in the range of Reynolds numbers (based on the tube diameter) from 360 to 1115. The results show that the lift is of the same order of magnitude as the drag, in fact, the drag to lift ratio was approximately equal to 2.

Further evidence of the existence of a significant lift force was recently reported. During an investigation of the head loss in pumping a slurry of fine glass spheres, Young (6) observed a "coring" phenomenon. For upward flow, the particles gathered toward the tube axis leaving a clear annulus of fluid next to the tube wall. This behavior was most prominent near the transition between laminar and turbulent flow. The lateral or lift force responsible for the phenomenon was assumed to be due to the nonuniform free stream since a velocity gradient exists near the wall of a pipe.

Rubinow and Keller (7) have calculated the lift acting on a spinning sphere moving with a velocity $\vec{V}$ for

Reynolds numbers less than one. Their equation in vector form is

$$L = \pi r^3 \rho_f \vec{\Omega} \times \vec{V} [1 + O(N)]$$

where r is the sphere radius, $\vec{\Omega}$ is the angular velocity, and O(N) is the order of Reynolds number. The first term on the right shows that the lift is independent of viscosity. No experimental verification was undertaken.

DEVELOPMENT OF EXPERIMENTAL PARAMETERS

General Description of Particle Behavior

A sphere, when released from rest in a still viscous fluid contained in a closed circular tube inclined at an angle θ from a vertical position, will accelerate under the influence of gravity until it reaches a terminal velocity. During the acceleration, a resisting fluid force acting on the sphere increases until it equals the component of the sphere's weight in the direction of motion. From this point of equalization the sphere effectively moves at a constant velocity.

In the case of this investigation, a particular set of conditions was found in which a sphere followed a rectilinear path without rotation at a constant distance from the tube wall during its constant velocity interval. With all other variables held constant, an increase in the angle of inclination with the vertical caused a decrease in terminal velocity. However, the range of angles in which the sphere moved in equilibrium was approximately four degrees. As is shown in Figure 1, each of the four regions of angles has a characteristic type of motion. Region A contains all angles greater than the lift-off angle wherein the sphere simply rolls on the tube wall. As the lift-off angle is approached,

Figure 1. Types of motion as a function of inclination angle

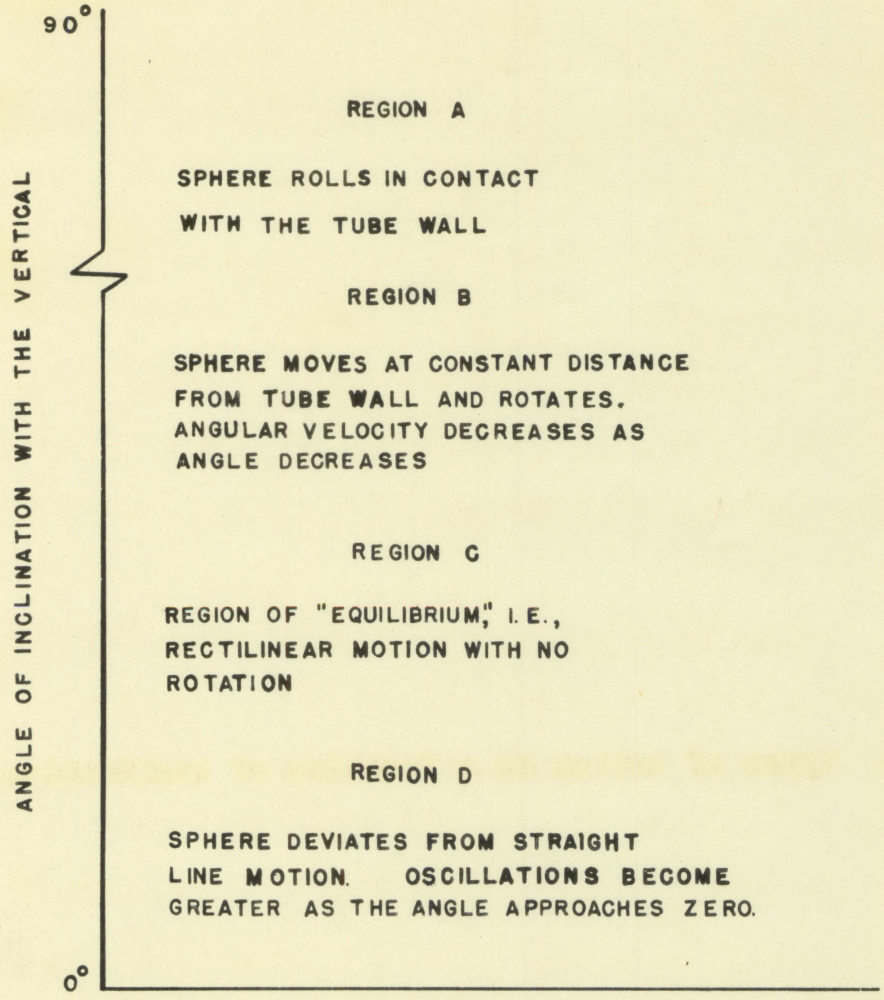
90°
ANGLE OF INCLINATION WITH THE VERTICAL
REGION A
SPHERE ROLLS IN CONTACT WITH THE TUBE WALL
REGION B
SPHERE MOVES AT CONSTANT DISTANCE FROM TUBE WALL AND ROTATES. ANGULAR VELOCITY DECREASES AS ANGLE DECREASES
REGION C
REGION OF "EQUILIBRIUM," I.E., RECTILINEAR MOTION WITH NO ROTATION
REGION D
SPHERE DEVIATES FROM STRAIGHT LINE MOTION. OSCILLATIONS BECOME GREATER AS THE ANGLE APPROACHES ZERO.
0°

the sphere has a tendency to jump off the wall and settle back quickly.

In region B, the sphere moves essentially at a constant distance from the tube wall while rotating about a horizontal axis through its center, perpendicular to the direction of motion. The direction of rotation is opposite that of the rolling sphere in region A. The angular velocity of the sphere decreases as the tube is inclined at successively smaller angles. The transition from region A to region B is quite distinct in that less than one-half degree separates the two types of motion.

Region C, which shall be referred to as the equilibrium region, is characterized by a small range of angles ($\Delta\theta \sim 4^{\circ}$) in which the sphere follows a rectilinear path and has no rotation.

In the range of angles defined as region D, the sphere does not follow a straight line path, but oscillates laterally about its average line of motion. The oscillations increase in amplitude and frequency as the tube approaches a vertical position.

Measurement of Fluid Forces

The condition of equilibrium described above allows the indirect measurement of the fluid force acting on the

sphere. The force system is shown in the free-body diagram of the sphere in its equilibrium condition in Figure 2. The resultant fluid force is decomposed into two components, one parallel to the direction of motion, called the drag F, and the other at right angles to the motion which is designated as the lift L. The resultant fluid force represents the integrated normal and tangential fluid forces on all incremental surface elements of the sphere. The weight of the sphere in the fluid is denoted by W' and is equal to the weight of the sphere minus the buoyant force.

The equilibrium equations for the sphere are

$$L = W' \sin \theta \tag{2}$$

in the n-direction, and

$$F = W' \cos \theta \tag{3}$$

in the t-direction.

Since W' and θ are easily determined, the lift can be measured by using the relationship in Equation 2. This measurement has the advantage that attachments to the sphere are not required. In addition, if it is assumed that the sphere is stationary with respect to the tube wall and the fluid moving past the sphere, there is no velocity gradient associated with the fluid far from the sphere.

One disadvantage of this method is if all other

Figure 2. Free-body diagram of sphere

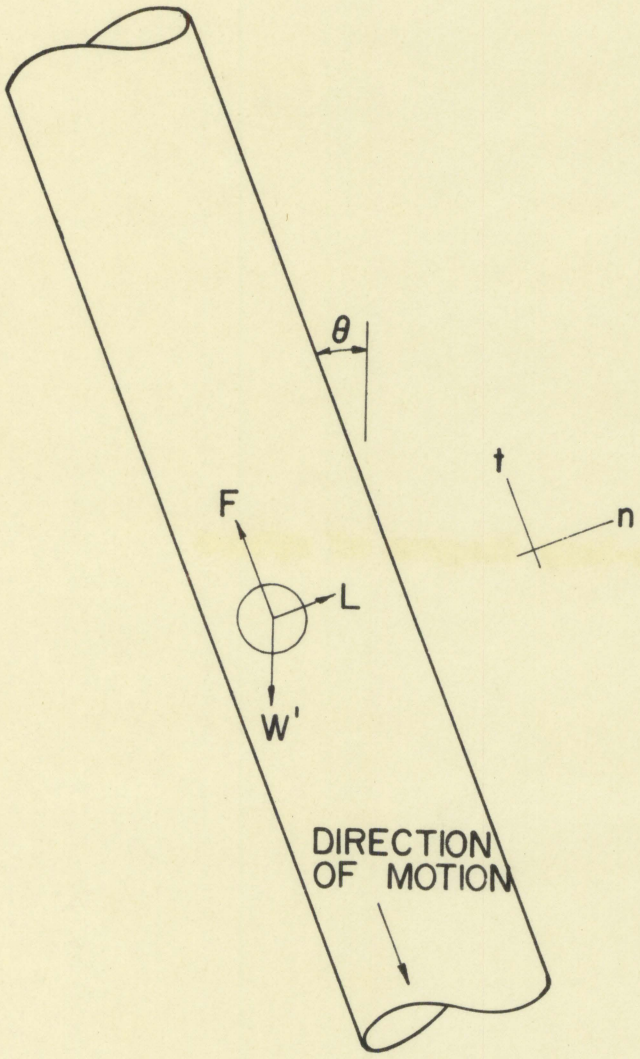
θ
t
n
F
L
W'
DIRECTION
OF MOTION

conditions are held constant, the velocity of the particle can be varied only by changing the inclination of the tube.

Choice of Variables

The lift coefficient, defined in Equation 1, is known to be a function of many variables. In this investigation the choice of variables was based on the total system of sphere, tube, and fluid. The geometry, fluid and particle properties, and the force system were taken into consideration. The variables which were assumed to have an influence on the lift coefficient are listed in Table 1 with their symbols and dimensions in the FLT system, where F = force
L = length
T = time

Table 1. List of variables influencing the lift coefficient

Symbol	Variable	Dimension
C_L	Lift coefficient	$F^0 L^0 T^0$
d	Sphere diameter	L
D	Tube diameter	L
θ	Inclination angle	$F^0 L^0 T^0$
μ	Viscosity	$F T L^{-2}$
ρ_f	Fluid density	$F T^2 L^{-4}$
ρ_s	Sphere density	$F T^2 L^{-4}$
g	Acceleration of gravity	$L T^{-2}$

The coefficient of lift as a function of the independent variables may be written in the form

$$C_L = \phi_1\left[d, D, \theta, \mu, \rho_f, \rho_s, g\right] \tag{4}$$

The velocity is not included among the variables since it is a derived term, i.e., once the independent variables are fixed, the velocity is determined. The lift is also omitted for the same reason.

The methods of dimensional analysis, as outlined in Murphy (8), were used to form dimensionless ratios or Pi terms and to establish a functional relationship between them.

According to the Buckinghan Pi Theorem, the number of dimensionless and independent terms needed to relate the variables in any one phenomenon is equal to the number of terms involved minus the number of dimensions in which those terms are measured.

In the list of variables, eight terms are involved, and these may be measured in three dimensions. Therefore, five dimensionless and independent Pi terms are required. These Pi terms are expressed in a form relating the dependent variable π_1 with the independent variables. Hence,

$$\pi_1 = F(\pi_2, \pi_3, \pi_4, \pi_5) . \tag{5}$$

One possible arrangement is

$$\pi_1 = C_L \qquad \pi_4 = \frac{d}{D}$$

$$\pi_2 = \sin\theta \qquad \pi_5 = \frac{\rho_s}{\rho_f}$$

$$\pi_3 = \frac{\mu^2}{\rho_s^2 g d^3}$$

where each term is dimensionless and independent. Throughout this thesis the symbol π with subscripts one through five is used to designate the dimensionless quantities just listed.

Equation 4 written in the form of Equation 5 gives

$$C_L = \phi_2\left[\sin\theta, \frac{\mu^2}{\rho_s^2 g d^3}, \frac{d}{D}, \frac{\rho_s}{\rho_f}\right] \qquad (6)$$

Suitability of Pi Terms to Experimental Determination

One advantage of using the methods of dimensional analysis was the reduction of the number of variables which had to be investigated in the experiment. The experiment, in order to take greatest advantage of the form of Equation 5, was designed so that all of the Pi terms in the function except one were held constant, and the remaining one was varied to establish a relationship between it and π_1. Repeating this procedure for all the Pi terms in the function yielded relationships between π_1 and the other Pi terms.

Finally, correlation of these relationships resulted in a general relationship for the phenomenon.

Examination of the independent Pi terms shows that all except π_5 may be individually varied while the remaining terms are held constant. Since π_3 was varied by changing the fluid temperature, the density ratio, denoted by π_5, would also change. However, the change in π_5 was so small that it was neglected. Further concern with π_5 as a variable was eliminated since the sphere and fluid were not changed during the experiment. The π_4 term was varied by using five tubes of differing diameters.

EXPERIMENTAL INVESTIGATION

At the earliest stage of this investigation, the need for precise measurements became evident because the range of variables was limited due to the restricted region in which the sphere moved in equilibrium. The contribution of the errors in each of the measured quantities to the overall error in the determination of the lift coefficient was analyzed. This analysis aided in the design of the experimental equipment and procedures by pointing out the measurements which had to be most precise.

Materials

The fluid

The fluid used throughout the experiment was distilled water. Difficulty encountered in obtaining consistent values of sphere velocity was found to be primarily due to small bits of material in fiber form present in the fluid. These fibers were first observed on the sphere with the aid of a microscope. The nature of the foreign matter was not analytically determined, but it was assumed to be ordinary lint or dust. The adoption of careful procedures for cleaning the test apparatus and for filtering the water reduced the contamination and improved the consistency of the velocity

measurements.

The sphere

It was anticipated that the magnitude of the lift would be small. Therefore, a material of low specific gravity was needed.

A sphere made of nylon was used in the experiment because of the following properties (9, p. 795):

1. The specific gravity of nylon (Sp. gr. = 1.14) is slightly greater than water.
2. Nylon is chemically inert in water.
3. Physical size changes, i.e., swelling due to water absorbtion and temperature variation, would be insignificant in the experiment.

Only one sphere was used because the introduction of surface roughness as a variable was undesirable. Measurements performed using apparently identical 3/32-inch-diameter spheres showed a 15% difference in velocity data under identical conditions. The difference in surface conditions was assumed to be responsible for the discrepancy.

Table 2. Physical properties of the sphere

Sphere diameter[a]	Weight[b]	Density
0.1291 ± 0.0001 in.	$(4.437 \pm 0.009) 10^{-5}$ lb	2.206 slugs/ft^3

[a]Measured with Gaertner Toolmaker's Microscope.

[b]Measured with Ainsworth Analytical Balance.

Tubes

All five tubes used in the experiment were Pyrex glass of circular cross section and approximately 50 inches in length. The tubes were visually selected for axial straightness. A 1/4 inch section cut from either end was measured for the diameter determination.

Table 3. List of tube diameters

Designation	Tube diameter[a]
T_1	0.3960 in.
T_2	0.4536 in.
T_3	0.5724 in.
T_4	0.6803 in.
T_5	0.8646 in.

[a]Measured with Gaertner Toolmaker's Microscope.

Apparatus

A schematic diagram of the experimental equipment is shown in Figure 3. The experimental tube was mounted concentrically within a 1-15/32 inch inside diameter glass water jacket capable of maintaining the test section within ± 0.25 degree Centigrade along the axis at steady state

Figure 3. Schematic diagram of the experimental apparatus

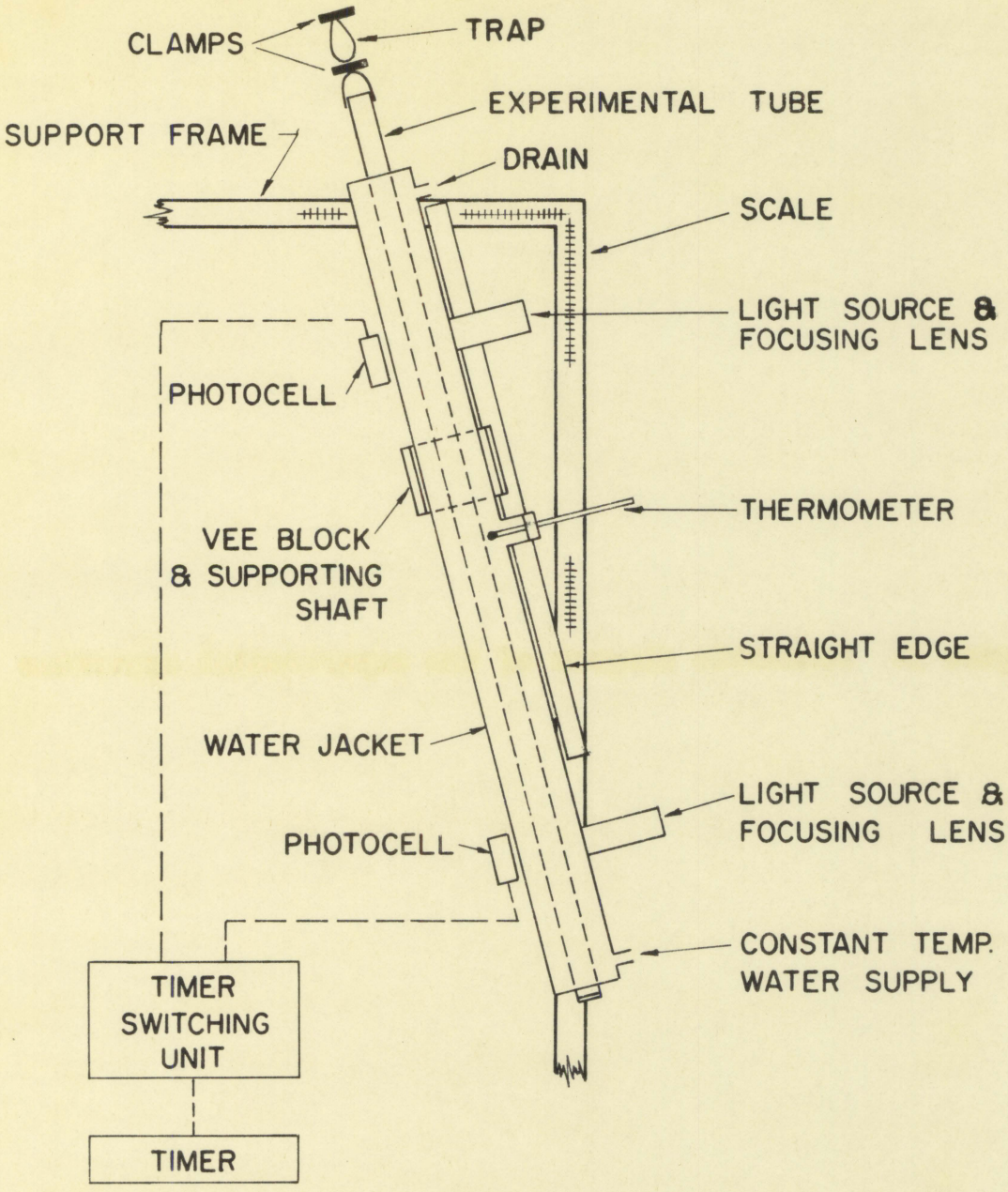
CLAMPS
TRAP
EXPERIMENTAL TUBE
SUPPORT FRAME
DRAIN
SCALE
LIGHT SOURCE & FOCUSING LENS
PHOTOCELL
THERMOMETER
VEE BLOCK & SUPPORTING SHAFT
STRAIGHT EDGE
WATER JACKET
LIGHT SOURCE & FOCUSING LENS
PHOTOCELL
CONSTANT TEMP. WATER SUPPLY
TIMER SWITCHING UNIT
TIMER

operation. The feed water was piped to the jacket from hot and cold water taps through a mixing junction. A bubble trap was installed between the mixer and the entrance to the lower end of the jacket to prevent bubbles from actuating the timing mechanism. Effluent water was piped to a drain. Fluid temperature readings were measured with a partial-immersion mercury thermometer positioned mid-way along the axis of the tube.

Velocity data were obtained from "time-of-flight" measurements. The two light beam sources were mounted on the water jacket 2.577 ± 0.0002 feet apart. This distance was determined, after mounting, with a cathetometer. Photocells were mounted directly opposite the sources. The light beam source shown in Figure 4 consisted of #44 light bulb and two positive lenses. The lens system and bulb were adjustable so that the light beam could be sharply focused. When the top photocell was activated by the sphere crossing the light beam, the switching unit started the timer. The timer was stopped when the bottom light beam was interrupted by the passage of the sphere. The switching unit circuit diagram is shown in Figure 6. A scaler normally used in radiation detection measurements was modified to serve as the timer. Since the test mode of the scaler utilized 60 cycle line frequency, the decade display could be read to one-sixtieth of a second.

Figure 4. Schematic diagram of light beam source and photocell arrangement

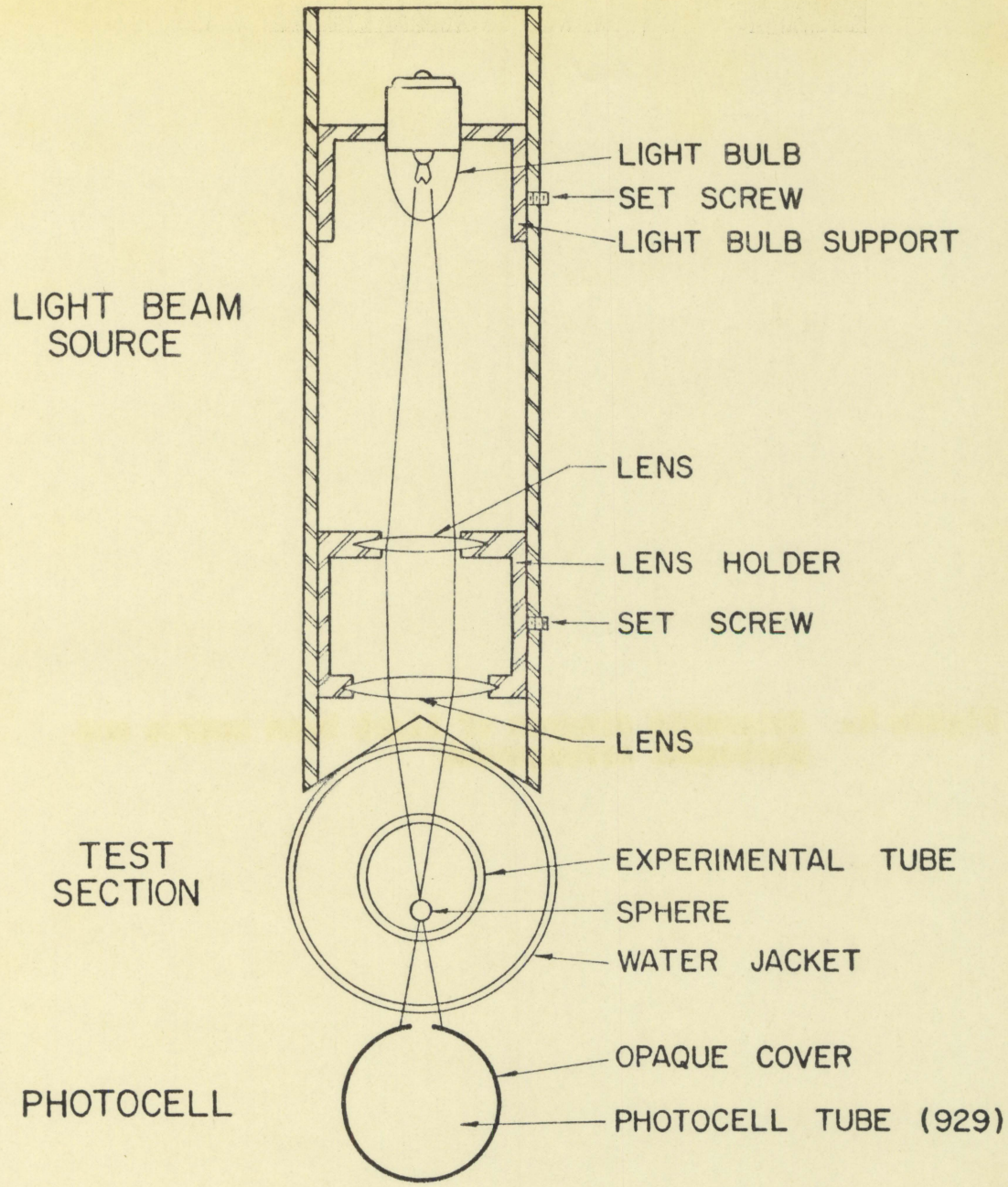
LIGHT BULB
SET SCREW
LIGHT BULB SUPPORT
LIGHT BEAM SOURCE
LENS
LENS HOLDER
SET SCREW
LENS
TEST SECTION
EXPERIMENTAL TUBE
SPHERE
WATER JACKET
OPAQUE COVER
PHOTOCELL
PHOTOCELL TUBE (929)

Figure 5. The experimental apparatus

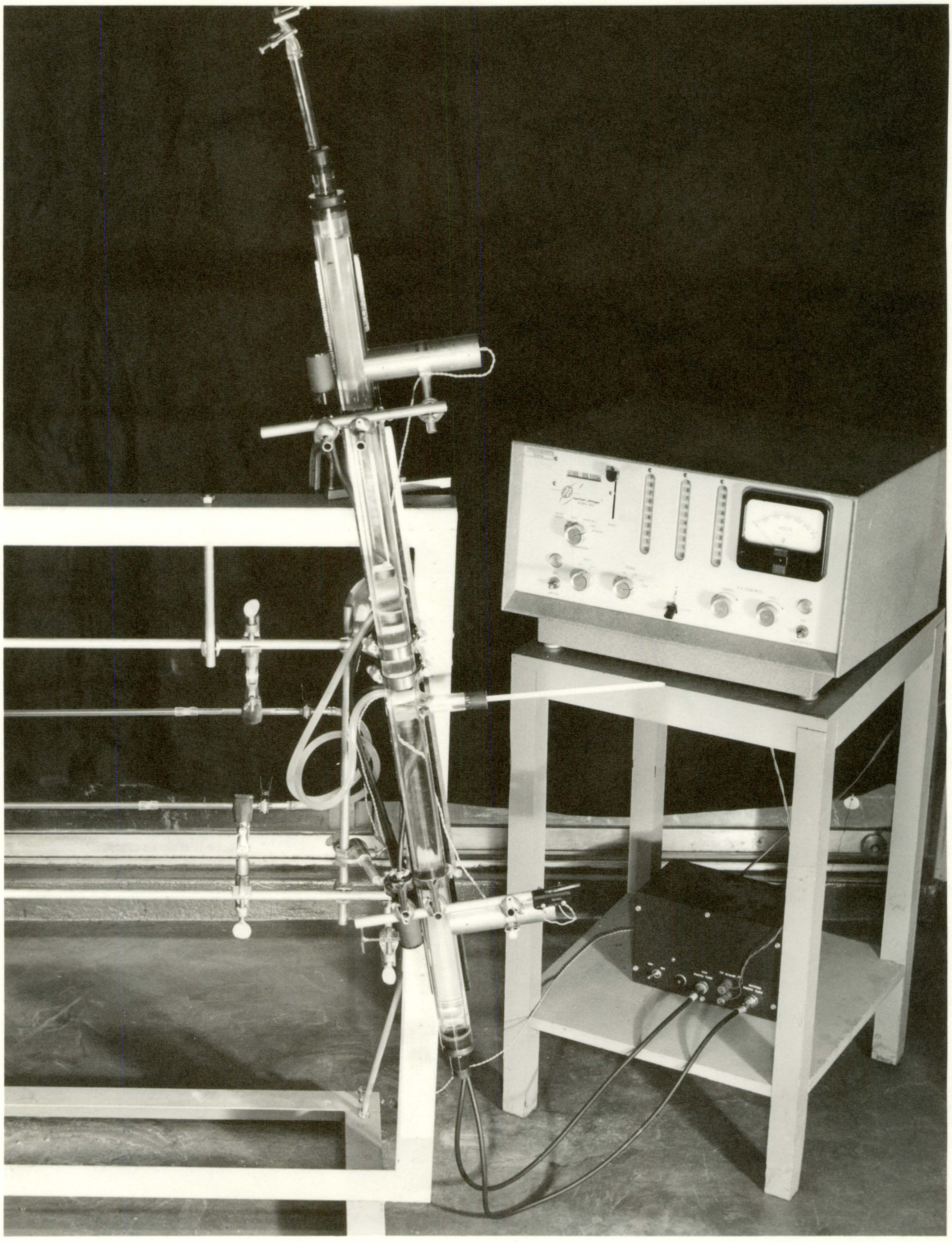

Figure 6. Circuit diagram of timer switching unit

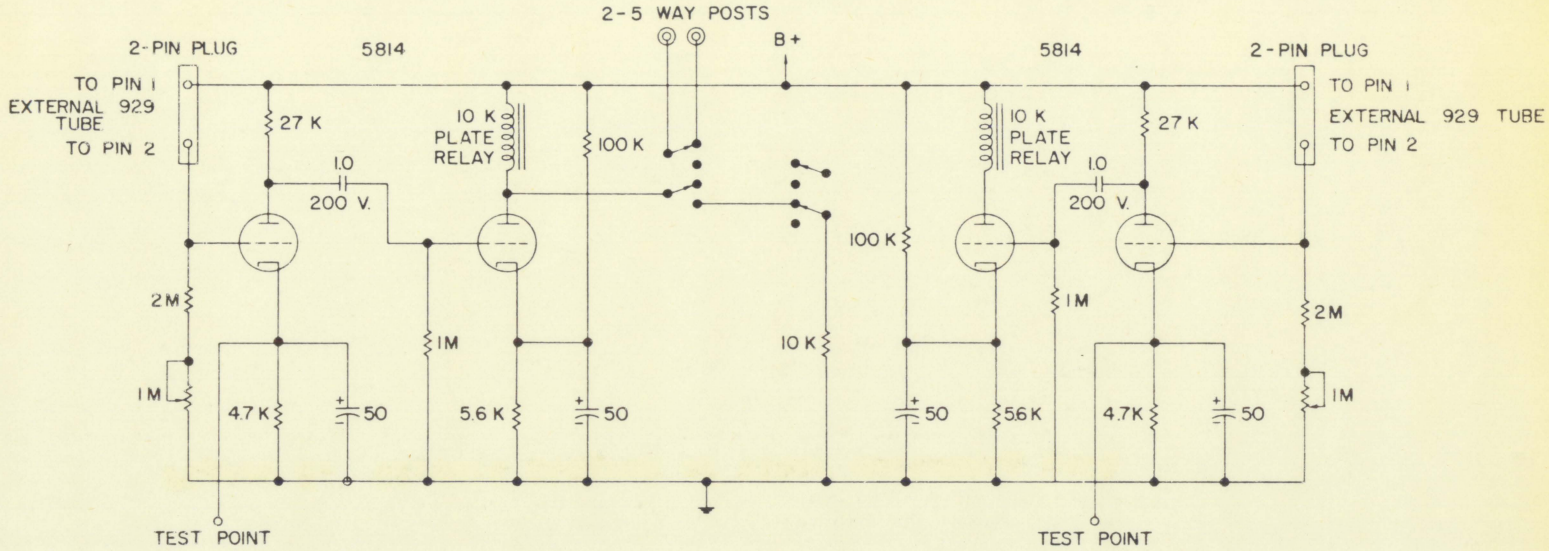
2-5 WAY POSTS
B+
2-PIN PLUG
5814
5814
2-PIN PLUG
TO PIN 1
EXTERNAL 929 TUBE
TO PIN 2
27 K
1.0
200 V.
10 K
PLATE
RELAY
100 K
100 K
10 K
PLATE
RELAY
1.0
200 V.
27 K
TO PIN 1
EXTERNAL 929 TUBE
TO PIN 2
2M
1M
4.7 K
50
1M
5.6 K
50
10 K
50
5.6 K
1M
4.7K
50
2M
1M
TEST POINT
TEST POINT

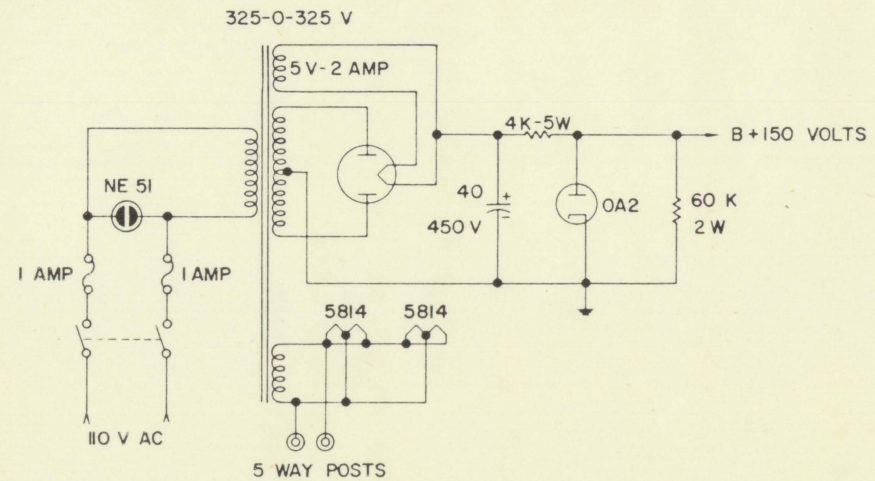
325-0-325 V
5 V-2 AMP
4K-5W
B+150 VOLTS
NE 51
40
450 V
0A2
60 K
2 W
1 AMP
1 AMP
5814
5814
110 V AC
5 WAY POSTS

Several repetitions of the velocity measurements were necessary due to statistical fluctuations in the data. Therefore, the water jacket was mounted on a vee block and shaft which could be rotated 360 degrees. This made it possible to return the sphere to its starting position and reposition the tube for the next run. The trap at the top of the tube served two purposes. It allowed the tube to be completely filled so that air bubbles were not present in the tube, and it also acted as a holding chamber for the sphere until the lower clamp was released to begin the next run.

The shaft mentioned above passed through a bearing which was attached to a rigid metal frame. Plumb and level adjustments were built into the supporting structure.

The angle of inclination was determined by measuring the legs of the triangle formed by the intersection of a straight edge attached to the test section and two sides of the frame which were joined with a 90 degree angle between them.

Procedure

Alignment of the test section

Before the start of a test and while the experimental tube was empty, a wire was dropped through the tube and then connected to a weight to plumb the test section. The metal

frame to which the test section was attached was also plumbed and leveled. This procedure was necessary to insure that the plane of rotation of the tube was parallel to the plane of the support frame. Next, the straight edge was checked and adjusted for alignment with the vertical scale on the metal frame. These adjustments held throughout the series of runs until the experimental tube was removed and replaced.

Preparation of materials

The discovery of the small dust particles in the distilled water necessitated routine filtering of the test fluid. A medium grade Büchner-type funnel was used as the filter and proved to be satisfactory. The experimental tube was thoroughly scrubbed with a detergent solution, rinsed with filtered water, filled immediately, and sealed.

The sphere was examined for dust fibers and cleaned under a 100 x binocular microscope before it was inserted into the experimental tube. A series of indelible ink dots were applied to the surface of the sphere to aid the visual check for rotation. The sphere was placed in the trap and released by loosening the lower clamp. With the clamp in the release position, the trap was filled to the top. Then the upper clamp was tightened so that excess water spilled out and the trap was completely filled and free of air bubbles. The water jacket feed was turned on and allowed to come to a

selected steady state temperature.

The top gate (light beam source and photocell) was positioned at a distance from the release point where the sphere was moving at terminal velocity. This distance was experimentally determined by measuring the average velocity of the sphere through five six-inch intervals. The lower gate was mounted one foot from the bottom of the tube. It was assumed that the end of the tube would not have an influence on the sphere at this distance.

Performing the experiment

The experiment was designed and executed to test the variation of π_1 with π_2, π_3, and π_4 in turn, while the two remaining variables were held constant. The variation of π_1 with π_2 was determined while the fluid temperature and tube diameter were held constant. Velocity data were recorded at one-half degree increments of angle throughout the range of equilibrium. Data relating π_1 with π_3 were obtained by varying the fluid temperature from 15 to 30° C. in five degree steps and performing the velocity measurements at the same angles at each of these temperatures. The relationship between π_1 and π_4 was determined from identical tests in five different tubes. In some instances the sphere was not moving in equilibrium, and therefore the measurements were not performed.

The quantities measured directly during the tests were the angle, fluid temperature, and the time for the sphere to traverse a known distance. The time measurement was performed ten times at each angle of inclination. After each group of ten runs was completed, the standard deviation of an individual measurement was calculated. If the standard deviation exceeded one-thirtieth of a second, the sphere was removed from the tube and microscopically examined for foreign material adhering to its surface, since the presence of impurities strongly affected the precision of the measurements. The experimental tube was emptied, thoroughly washed and rinsed, and refilled with filtered, distilled water. It was not uncommon to repeat this procedure three or four times in order to reduce the standard deviation to the acceptable value.

Calculation of the Lift Coefficient and its Standard Error

A conservative estimate of the standard error in the measurement of the lift coefficient was calculated using the method of propagation of errors. If a function F is composed of n independent quantities each contributing a standard error σ_{x_i} to the total error σ_p, then the expression

$$\sigma_F^2 = \sum_{i=1}^{n} \left(\frac{\partial F}{\partial x_i}\right)^2 \sigma_{x_i}^2 \qquad (7)$$

may be used to calculate an estimate of the standard error of the function. In order to apply Equation 7, the lift coefficient must be expressed in terms of the independently measured quantities. The coefficient becomes

$$C_L = \frac{V_s (\rho_s - \rho_f) g \sin \theta}{\rho_f A \frac{V^2}{2}} \qquad (8)$$

when Equation 2, with $W' = V_s (\rho_s - \rho_f) g$, is substituted in Equation 1. Equation 8, written in terms of the independently measured quantities is

$$C_L = \frac{\frac{\pi d^3}{6} \left(\frac{6 m_s}{\pi d^3} - \rho_f\right) g \sin \theta}{\rho_f \frac{\pi d^2}{4} \frac{V^2}{2}}$$

or

$$C_L = \frac{8 m_s g \sin \theta}{\rho_f \pi d^2 v^2} - \frac{4 d g \sin \theta}{3 v^2} \qquad (9)$$

where m_s is the mass of the sphere. The standard error in the measurement of the lift coefficient is found by applying Equation 7. Hence,

$$\sigma_{C_L}^2 = \left[\frac{8\ g \sin\theta}{\rho_f\ \pi d^2\ v^2}\right]^2 \sigma_{m_s}^2 + \left[\frac{16\ m_s\ g \sin\theta}{\rho_f\ \pi d^3\ v^2} + \frac{4\ g \sin\theta}{3\ \pi v^2}\right]^2 \sigma_d^2$$

$$+ \left[\frac{16(m_s - \frac{\pi d^3}{6}\rho_f) g \sin\theta}{\rho_f\ \pi d^2\ v^3}\right]^2 \sigma_v^2 \qquad (10)$$

$$+ \left[\frac{8(m_s - \frac{\pi d^3}{6}\rho_f) g}{\rho_f\ \pi d^2\ v^2}\right]^2 \sigma_{\sin\theta}^2$$

The substitution of numerical values for the case, $\bar{\pi}_2 = 0.1436$, $\bar{\pi}_3 = 17{,}750$, and $\bar{\pi}_4 = 0.190$ in Equations 8 and 10 gives

$$C_L = 0.0943 \pm 0.0015$$

The percentage error of this measurement is 1.6%. A detailed development of the standard errors used in this calculation appears in the Appendix.

RESULTS

This section is divided into two parts. The first part concerns the experimental results and the component equations, and the second part is devoted to the correlation of these results into a general prediction equation.

Experimental Results and Component Equations

Figure 7 shows the variation of π_1 with π_2 for four different values of π_3. The π_4 term, which is the diameter ratio, was held constant at 0.190. The term

$$\pi_3 = \frac{\mu^2}{\rho_s^2 g d^3}$$

was varied by changing the temperature of the fluid in five degree steps starting at 15° C. and ending at 30° C. Each straight line on the graph, therefore, represents the variation of π_1 with π_2 while the remaining variables, π_3 and π_4, are held constant. The fifth Pi term, $\pi_5 = \frac{\rho_s}{\rho_f}$, was assumed to be constant through the entire experiment since the maximum fluid density change was 0.3 percent, and the sphere density was assumed to be constant. Figures 8 and 9 are similar to Figure 7. These represent π_1 as a function of π_2 and π_3 with the diameter ratio held constant at values of 0.226 and 0.285

Figure 7. Variation of w_1 with w_2 while $\bar{w}_4 = 0.190$

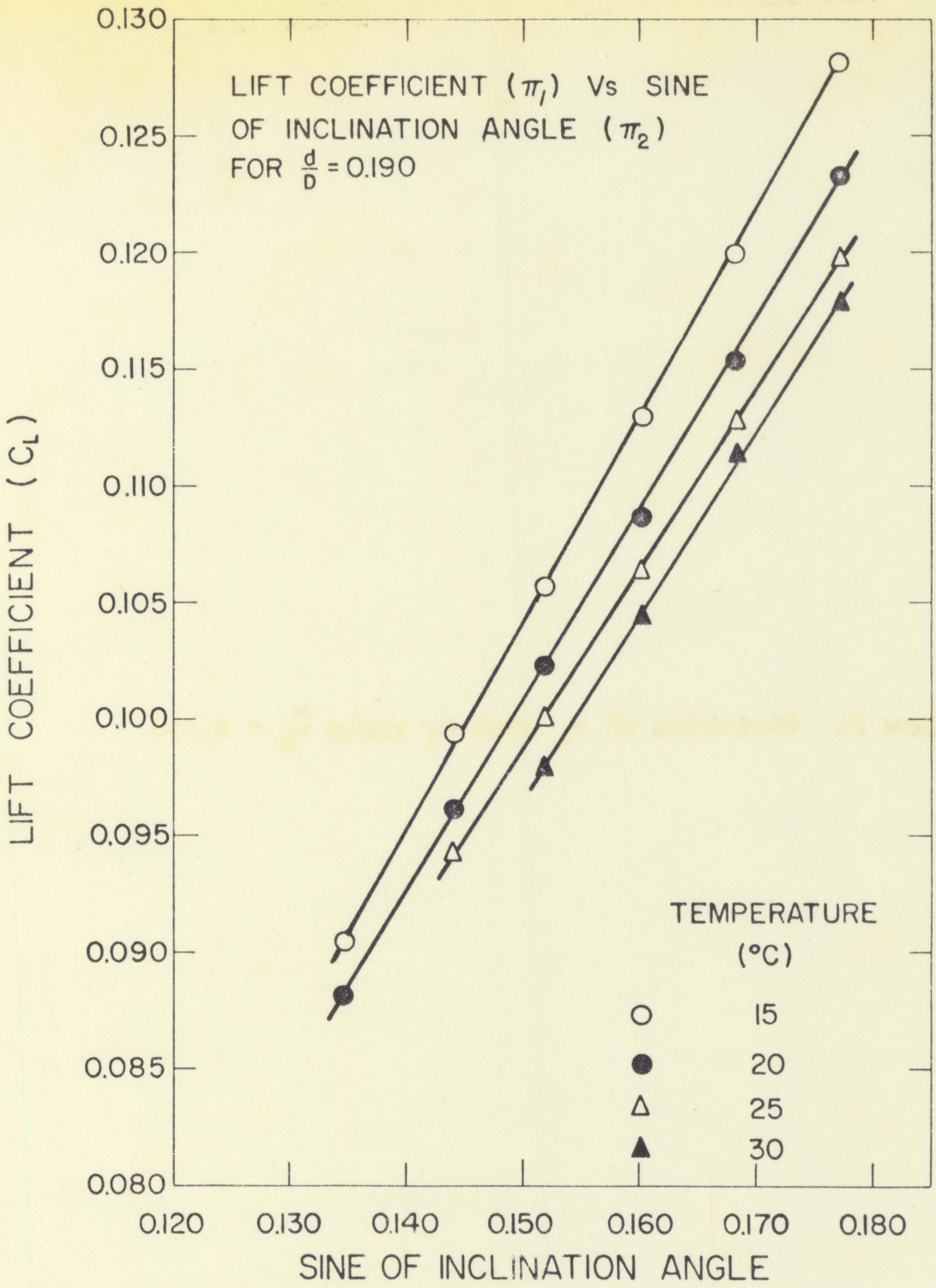
LIFT COEFFICIENT (π_1) Vs SINE OF INCLINATION ANGLE (π_2) FOR $\frac{d}{D}$ = 0.190
LIFT COEFFICIENT (C_L)
SINE OF INCLINATION ANGLE
0.130
0.125
0.120
0.115
0.110
0.105
0.100
0.095
0.090
0.085
0.080
0.120
0.130
0.140
0.150
0.160
0.170
0.180
TEMPERATURE (°C)
15
20
25
30

Figure 8. Variation of π_1 with π_2 while $\bar{\pi}_4 = 0.226$

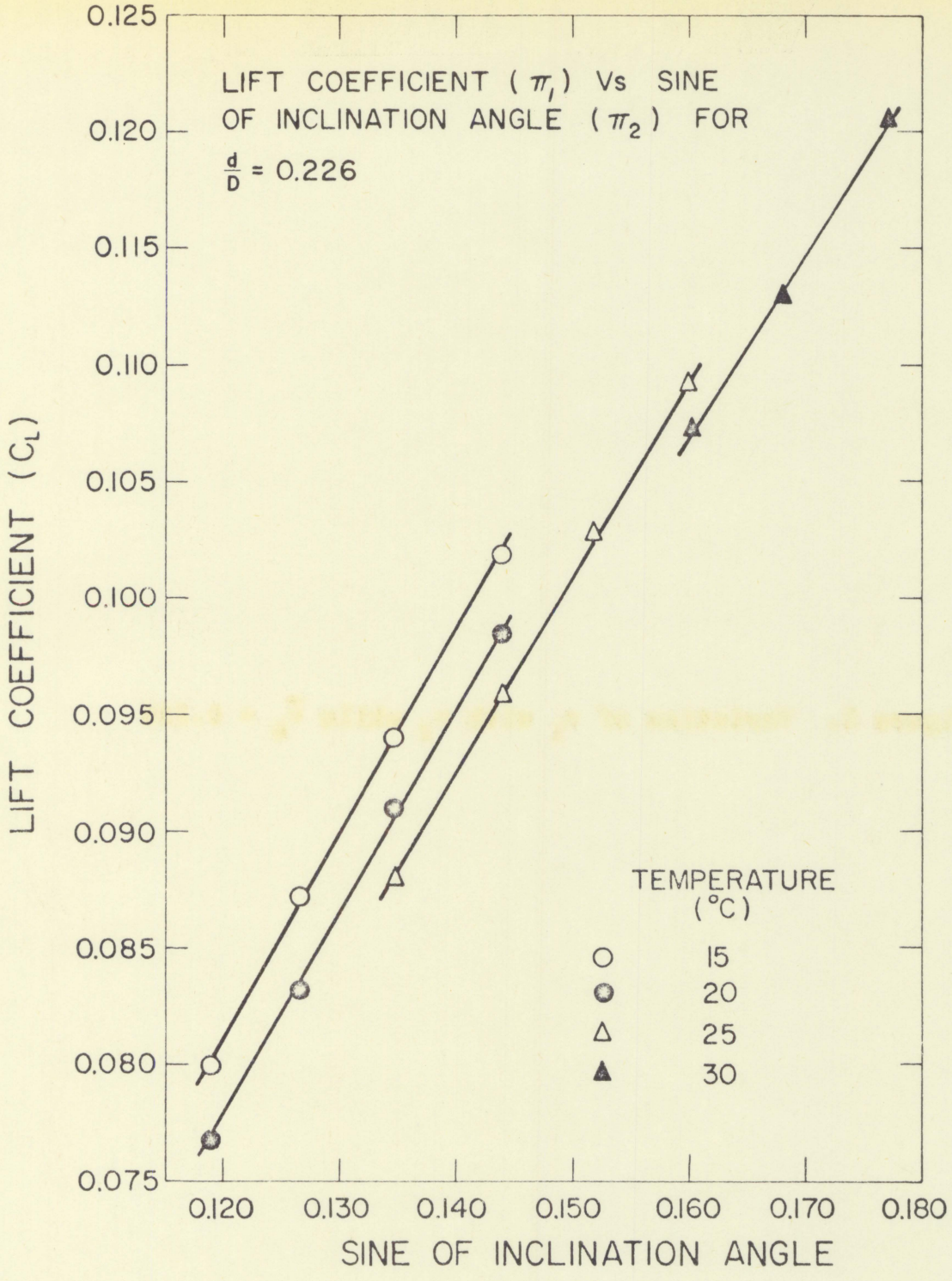
LIFT COEFFICIENT (π_1) Vs SINE OF INCLINATION ANGLE (π_2) FOR $\frac{d}{D}$ = 0.226
LIFT COEFFICIENT (C_L)
SINE OF INCLINATION ANGLE
0.125
0.120
0.115
0.110
0.105
0.100
0.095
0.090
0.085
0.080
0.075
0.120
0.130
0.140
0.150
0.160
0.170
0.180
TEMPERATURE (°C)
15
20
25
30

Figure 9. Variation of π_1 with π_2 while $\bar{\pi}_4 = 0.285$

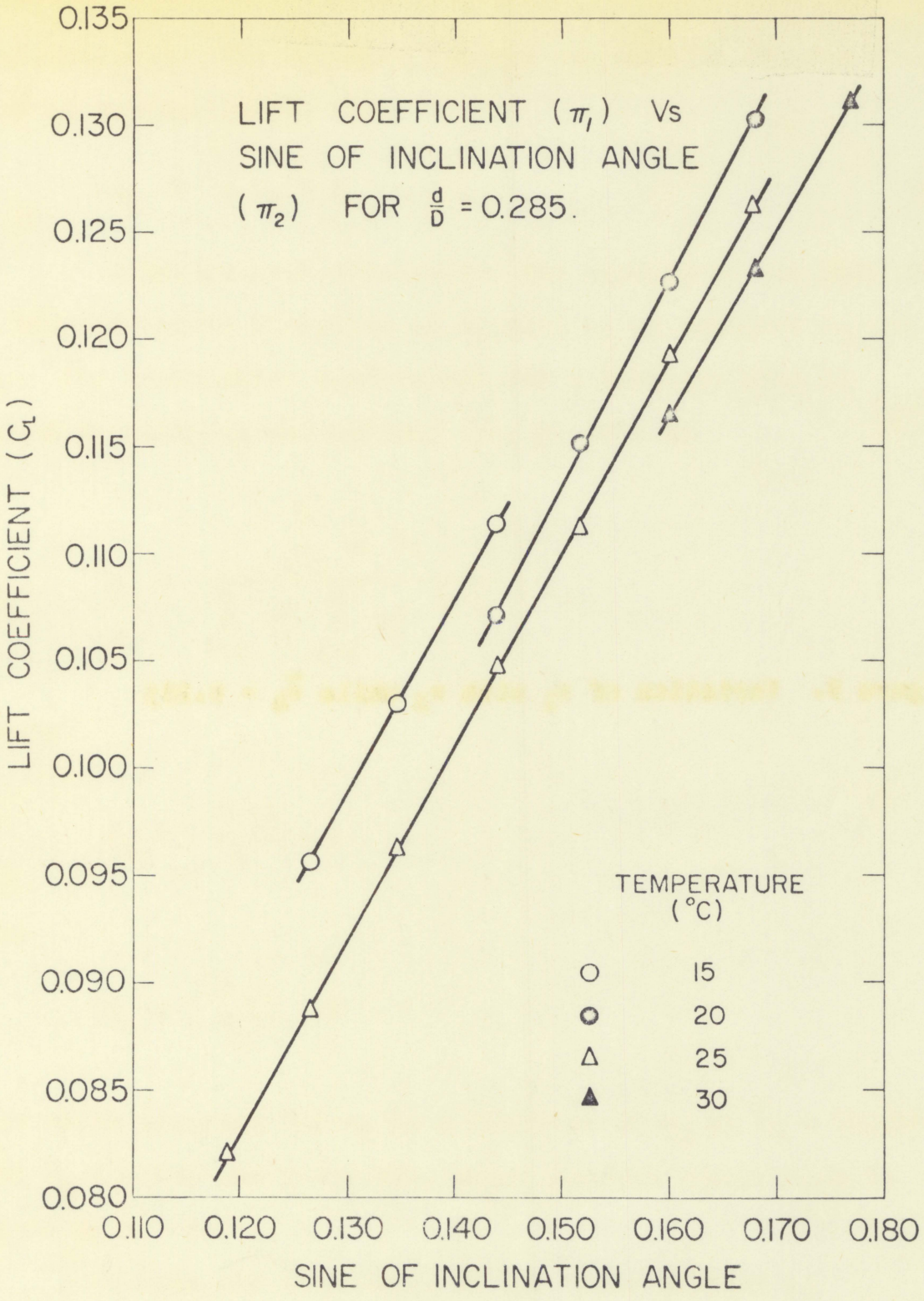
LIFT COEFFICIENT (π_1) Vs
SINE OF INCLINATION ANGLE
(π_2) FOR $\frac{d}{D}$ = 0.285.
LIFT COEFFICIENT (C_L)
SINE OF INCLINATION ANGLE
0.135
0.130
0.125
0.120
0.115
0.110
0.105
0.100
0.095
0.090
0.085
0.080
0.110
0.120
0.130
0.140
0.150
0.160
0.170
0.180
TEMPERATURE (°C)
15
20
25
30

respectively. The equation for any one line in Figures 7 - 9 may be written in the form

$$\pi_1 = B\,\pi_2 + A$$

A statistical correlation was applied to the data for a representative variation of π_1 with π_2 at constant π_3 and π_4. The correlation coefficient for a straight line is given by Worthing and Geffner (10, p. 284) as

$$r = \frac{\sum_{i=1}^{n} X_i Y_i}{\left[\sum_{i=1}^{n} X_i^2 \sum_{i=1}^{n} Y_i^2\right]^{1/2}}$$

where

$$X_i = \frac{\Sigma x_i}{n} - x$$

and

$$Y_i = \frac{\Sigma y_i}{n} - y$$

The value computed for π_1 as a function of π_2 at $\bar{\pi}_3 = 14{,}240$ and $\bar{\pi}_4 = 0.190$ was $r = 0.999$, where perfect correlation is given by $r = 1.000$.

Slopes and intercepts of the lines plotted in Figures 7 - 9 were calculated using the method of least

squares. The values are listed in Table 4. The standard errors assigned to the slopes and intercepts were calculated from the relationships given by Topping (11, p. 104)

$$\frac{\sigma_B^2}{n} = \frac{\sigma_A^2}{\Sigma x^2} = \frac{\sigma^2}{\Delta}$$

where

$$\sigma^2 = \frac{\Sigma\left[y_i - (A + Bx_i)\right]^2}{n - 2}$$

and

$$\Delta = n\,\Sigma x^2 - (\Sigma x)^2$$

The component equation chosen to represent the set of data, $\pi_1 = f_1(\pi_2, \bar{\pi}_3, \bar{\pi}_4)$ is

$$\pi_1 = 0.7663\,\pi_2 - 0.01596 \qquad (11)$$

with $\bar{\pi}_3 = 17{,}750$ and $\bar{\pi}_4 = 0.190$.

The data plotted in Figure 10 was taken from tests during which π_3 was varied, while π_2 and π_4 were held constant. The equation of an individual line is

$$\pi_1 = B'\,\pi_3 + A'$$

Slopes and intercepts of the lines were calculated and are

Figure 10. Variation of r_1 with r_3

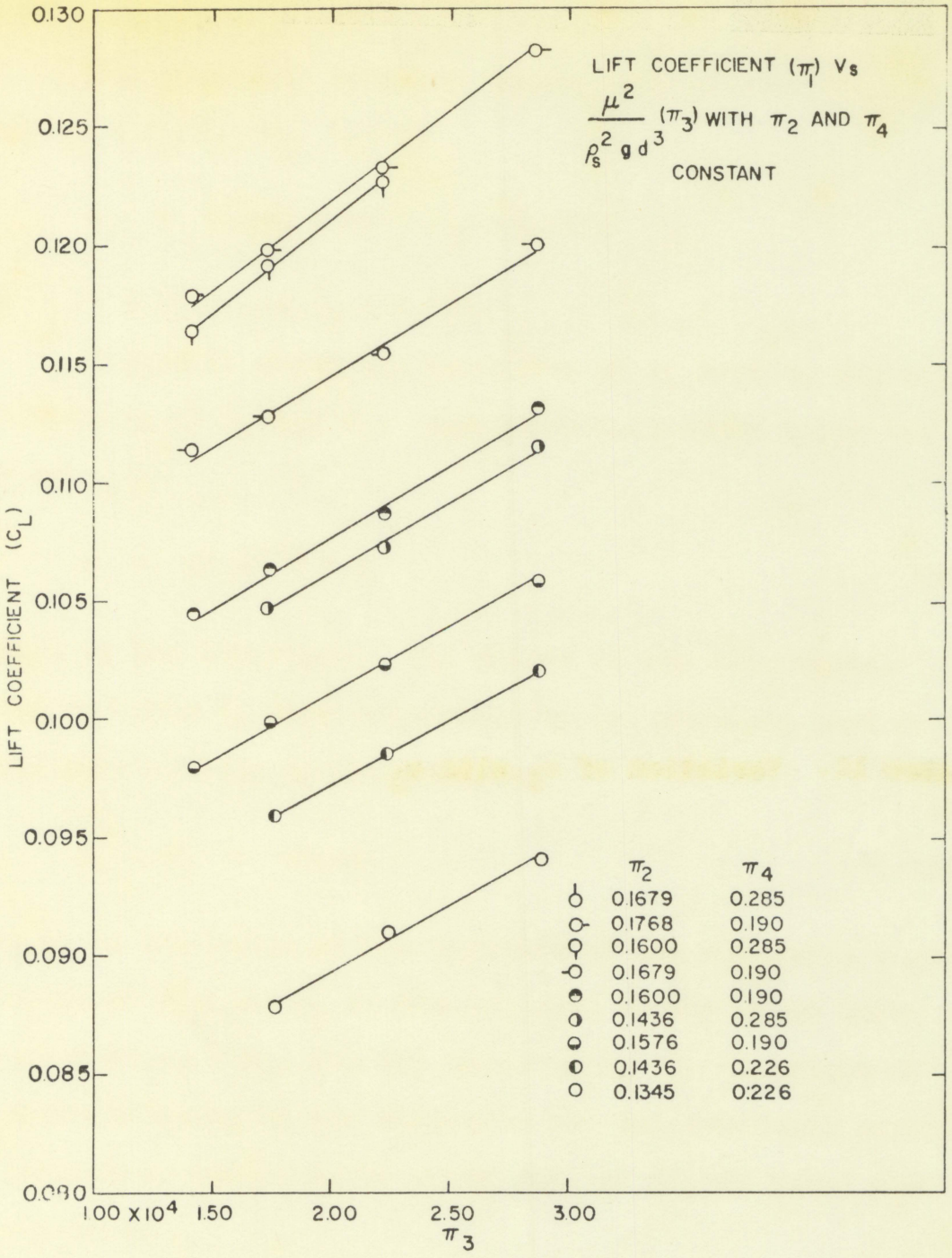
LIFT COEFFICIENT (π_1) Vs $\frac{\mu^2}{\rho_s^2 g d^3}$ (π_3) WITH π_2 AND π_4 CONSTANT
LIFT COEFFICIENT (C_L)
0.130
0.125
0.120
0.115
0.110
0.105
0.100
0.095
0.090
0.085
0.080
1.00 X10^4
1.50
2.00
2.50
3.00
π_3
π_2 π_4
0.1679 0.285
0.1768 0.190
0.1600 0.285
0.1679 0.190
0.1600 0.190
0.1436 0.285
0.1576 0.190
0.1436 0.226
0.1345 0.226

listed in Table 5.

The component equation chosen to represent the set of data, $\pi_1 = f_2(\bar{\pi}_2, \pi_3, \bar{\pi}_4)$ is

$$\pi_1 = 5.539 \times 10^{-7} \pi_3 + 0.0900 \qquad (12)$$

with $\bar{\pi}_2 = 0.1516$ and $\bar{\pi}_4 = 0.190$.

Figure 11 shows the variation of π_1 with π_4 for eight combinations of π_2 and π_3. Any individual curve takes the form of

$$y = A^* e^{B^* x} + E \qquad (13)$$

where E is the intercept. The values of the intercepts, listed in Table 6, were determined by (a) assuming that the curves were related by the equation

$$y_i - y_j = \text{const.} \qquad (14)$$

where y_i is the value of the ordinate of the reference curve evaluated at x_i, and y_j is the ordinate of any other curve evaluated at $x_j = x_i$, and (b) calculating the intercept of one curve to serve as the reference for the remaining curves. The intercept, according to Davis (12, p. 5), is found from the equation,

$$E = \frac{y_1 y_2 - (y_3^2)}{y_1 + y_2 - 2y_3}$$

Figure 11. Variation of π_1 with π_4

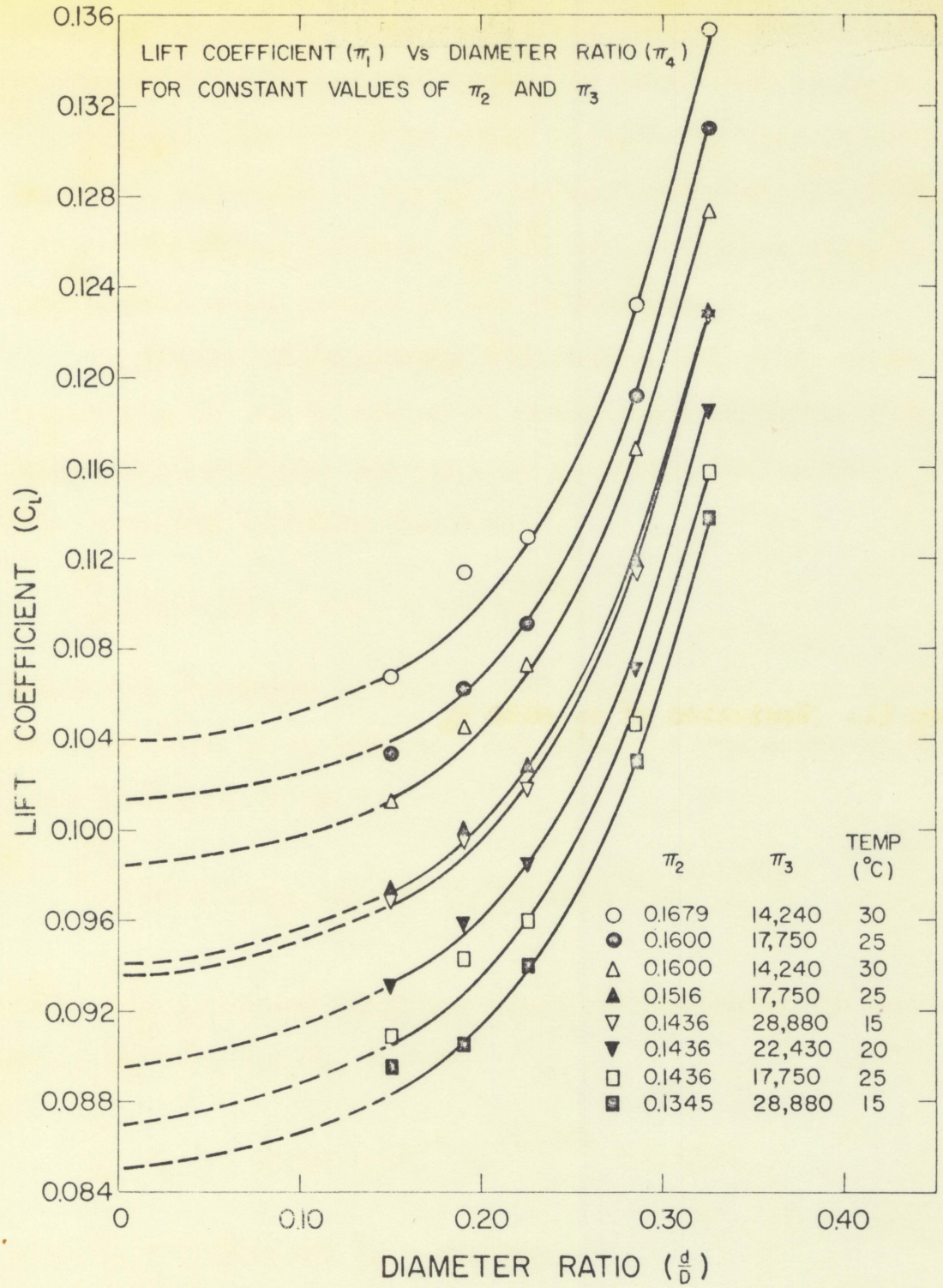
LIFT COEFFICIENT (π_1) Vs DIAMETER RATIO (π_4)
FOR CONSTANT VALUES OF π_2 AND π_3
LIFT COEFFICIENT (C_L)
DIAMETER RATIO ($\frac{d}{D}$)
0.136
0.132
0.128
0.124
0.120
0.116
0.112
0.108
0.104
0.100
0.096
0.092
0.088
0.084
0
0.10
0.20
0.30
0.40
π_2 π_3 TEMP (°C)
0.1679 14,240 30
0.1600 17,750 25
0.1600 14,240 30
0.1516 17,750 25
0.1436 28,880 15
0.1436 22,430 20
0.1436 17,750 25
0.1345 28,880 15

where the y_1 and y_2 values are determined from the extremities of the curve at x_1 and x_2, and y_3 is determined at $x_3 = (x_1 + x_2)/2$. It should be noted in assuming that Equation 14 is valid, the terms A" and B" become constants for all values of x. The dashed portions of the curves are the extrapolations from experimental points to the intercepts.

Figure 12 represents the natural log of π_1 minus the intercepts of the π_1 versus π_4 curves as a function of π_4. Regression technique was used to calculate the value of A" and B". Equation 13 takes the form

$$\pi_1 - E(\pi_2, \pi_3) = A'' e^{B''\pi_4} \qquad (15)$$

after the variables π_1 and π_4 are inserted and E is expressed as a function of π_2 and π_3. The equation representing the line in Figure 12 is

$$\pi_1 - E(\pi_2, \pi_3) = 5.362 \times 10^{-4} e^{12.33\pi_4} \qquad (16)$$

Thus, the component equation chosen to represent the set of data, $\pi_1 = f_3(\bar{\pi}_2, \bar{\pi}_3, \pi_4)$ is

$$\pi_1 = 5.362 \times 10^{-4} e^{12.33\pi_4} + 0.0940 \qquad (17)$$

with $\bar{\pi}_2 = 0.1516$ and $\bar{\pi}_3 = 17,750$.

Figure 12. $(\pi_1 - E)$ as a function of π_4

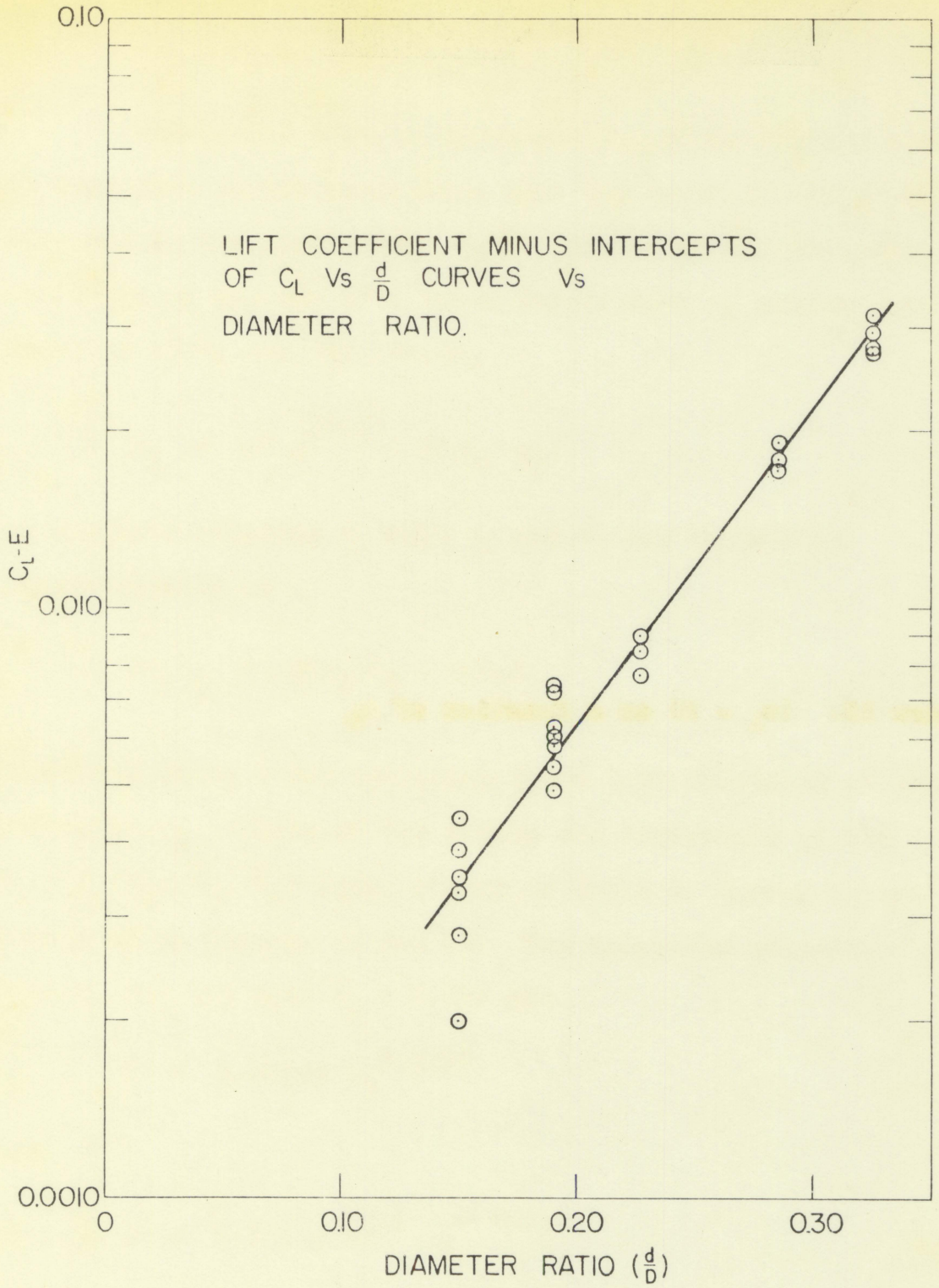
LIFT COEFFICIENT MINUS INTERCEPTS
OF C_L Vs $\frac{d}{D}$ CURVES Vs
DIAMETER RATIO.
C_L-E
0.10
0.010
0.0010
0
0.10
0.20
0.30
DIAMETER RATIO ($\frac{d}{D}$)

The Prediction Equation

The method used to correlate Equations 11, 12, and 17 is dependent on the assumption that the terms A" and B" in Equation 13 are constants. π_1 is related to the remaining variables by the sum of a known function of π_4 and an unknown function of π_2 and π_3. Hence,

$$\pi_1 = A'' e^{B''\pi_4} + E(\pi_2, \pi_3) \tag{18}$$

An equation relating π_1 with π_2 and π_3 may be written parametrically as

$$(\pi_1)_{\bar{\pi}_4} = C(\pi_3)\pi_2 - D(\pi_3) \tag{19}$$

where the slope C and intercept D are both functions of the parameter π_3. Plots of the slopes and intercepts of the $\pi_1 = f_1(\pi_2, \bar{\pi}_3, \bar{\pi}_4)$ data, listed in Table 4, versus π_3 are presented in Figures 13 and 14. The equations relating C and D to π_3 for the case $\bar{\pi}_4 = 0.226$ are

$$C = 0.08187\ \pi_3^{0.2607} \tag{20}$$

and

$$D = 4.671 \times 10^{-6}\ \pi_3^{0.8707} \tag{21}$$

The substitution of Equations 20 and 21 into Equation 19

Figure 13. Slope of ν_1 vs. sine θ data as a function of ν_3

Figure 14. Intercept of ν_1 vs. sine θ data as a function of ν_3

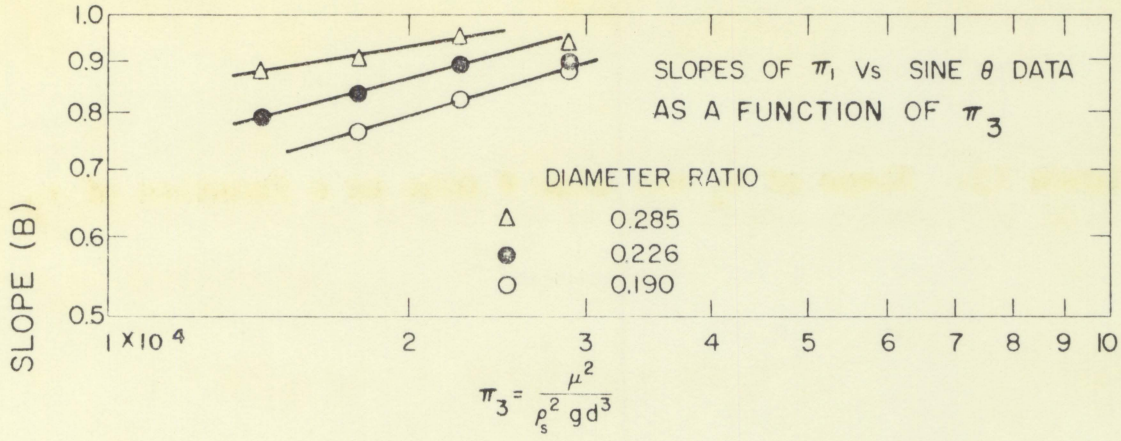
SLOPES OF π_1 Vs SINE θ DATA
AS A FUNCTION OF π_3
DIAMETER RATIO
0.285
0.226
0.190
SLOPE (B)
1.0
0.9
0.8
0.7
0.6
0.5
1 X 10 4
2
3
4
5
6
7
8
9
10
$\pi_3 = \frac{\mu^2}{\rho_s^2 g d^3}$

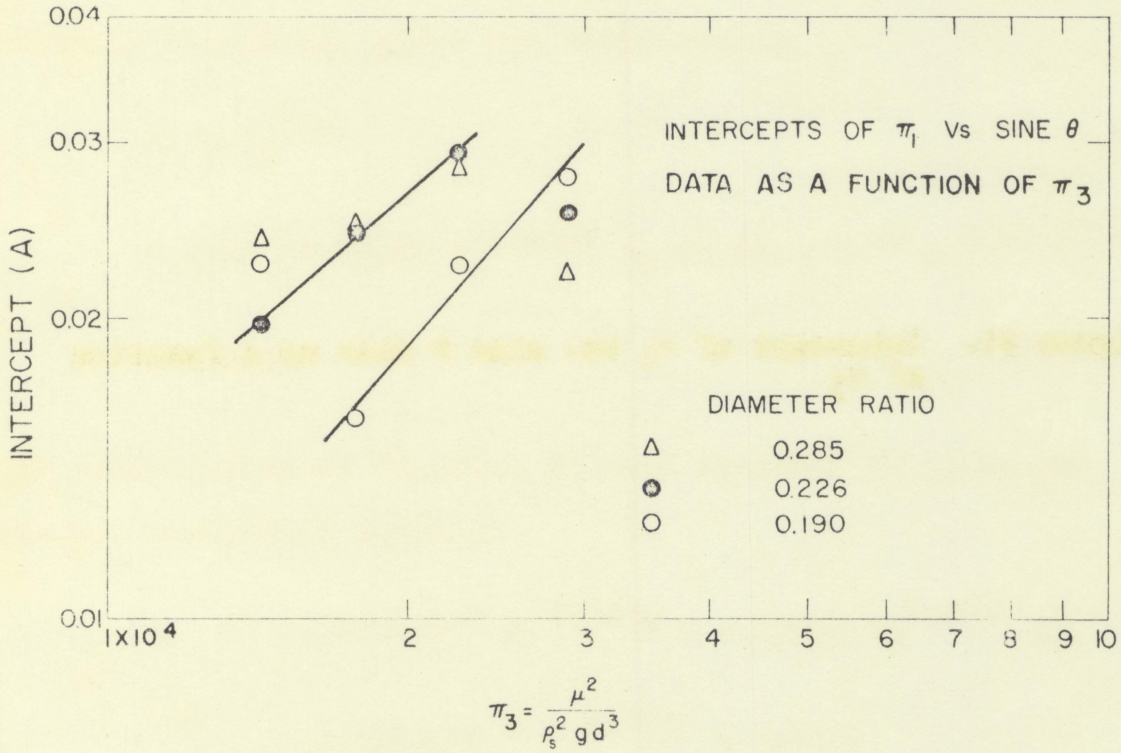
INTERCEPTS OF π_1 Vs SINE θ
DATA AS A FUNCTION OF π_3
DIAMETER RATIO
0.285
0.226
0.190
INTERCEPT (A)
0.04
0.03
0.02
0.01
1 X 10 4
2
3
4
5
6
7
8
9
10
$\pi_3 = \frac{\mu^2}{\rho_s^2 g d^3}$

yields

$$(\pi_1)_{\bar{\pi}_4} = 0.08187\ \pi_3^{0.2607}\ \pi_2 - 4.671 \times 10^{-6}\ \pi_3^{0.8707}$$

with $\bar{\pi}_4 = 0.226$. When $\bar{\pi}_4$ is substituted in Equation 18, the right hand sides of Equations 18 and 19 are equal, and they can be written as

$$K + E(\pi_2,\pi_3) = C(\pi_3)\ \pi_2 - D(\pi_3) \qquad (22)$$

A plot of $E(\pi_2,\pi_3)$ versus the right side of Equation 22, shown in Figure 15, gives the relationship

$$E(\pi_2,\pi_3) = \qquad (23)$$

$$0.8594\left[0.08187\ \pi_3^{0.2607}\ \pi_2 - 4.671 \times 10^{-6}\ \pi_3^{0.8707}\right]$$

$$- 0.0225$$

The substitution of Equation 23 into Equation 16 gives the general prediction equation

$$\pi_1 = 5.362 \times 10^{-4}\ e^{12.33\pi_4} + 0.07036\ \pi_3^{0.2607}\ \pi_2 \qquad (24)$$

$$- 4.014 \times 10^{-6}\ \pi_3^{0.8707} - 0.0225$$

A graphical representation of Equation 24 is not feasible due to the form of the equation. Comparisons of the

Figure 15. $E(n_2, n_3)$ versus $C(n_3)n_2 - D(n_3)$

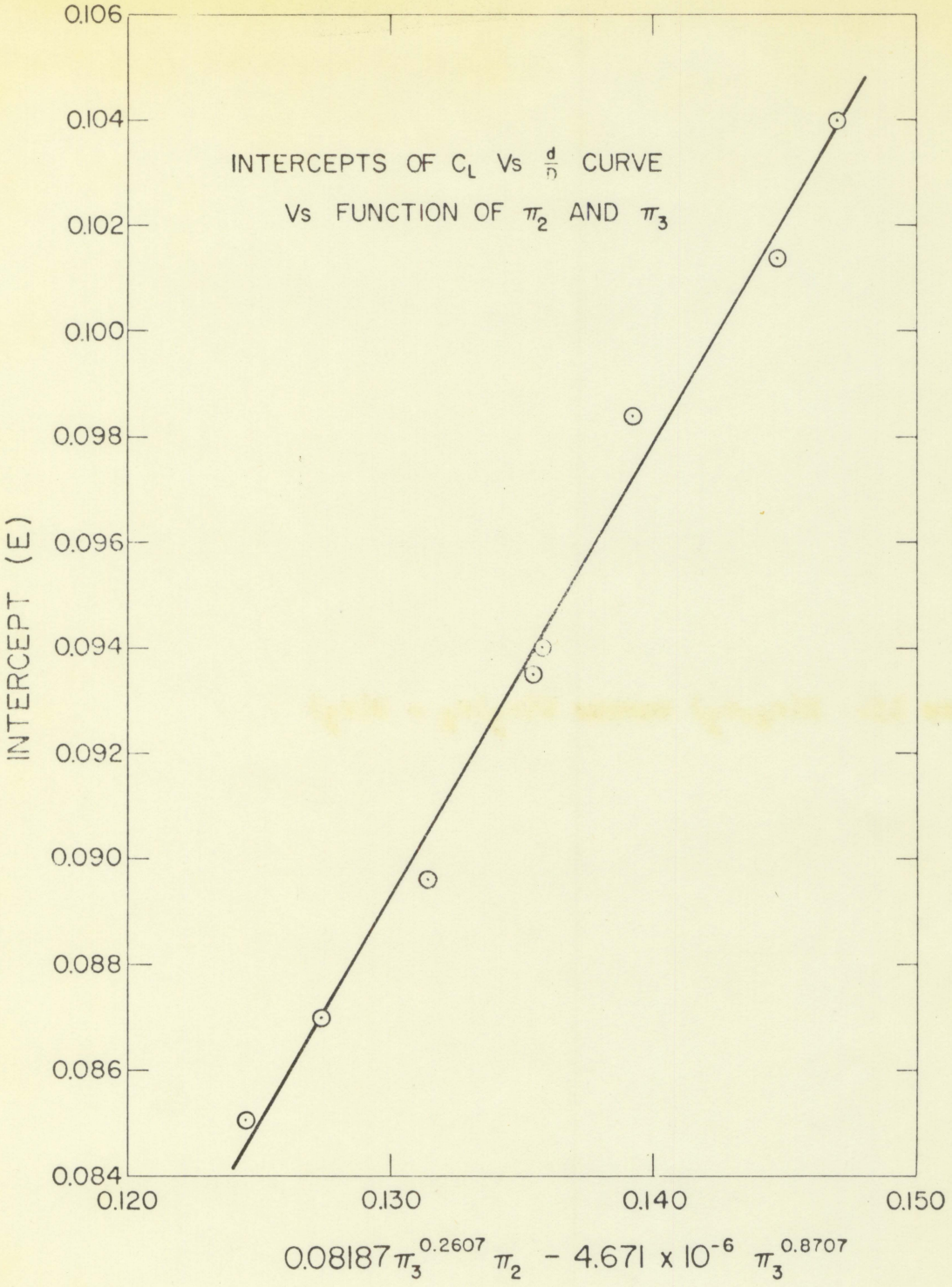
INTERCEPTS OF C_L Vs $\frac{d}{D}$ CURVE
Vs FUNCTION OF π_2 AND π_3
INTERCEPT (E)
0.106
0.104
0.102
0.100
0.098
0.096
0.094
0.092
0.090
0.088
0.086
0.084
0.120
0.130
0.140
0.150
$0.08187\pi_3^{0.2607}\pi_2 - 4.671 \times 10^{-6}\ \pi_3^{0.8707}$

experimental measurements and the values predicted by Equation 24 are listed in Table 7.

SUPPLEMENTARY ANALYSIS

In the section on development of experimental parameters the list of variables assumed to be pertinent to the problem did not include the velocity since it was a derived quantity. Thus, Equation 24 would be of limited use in application problems where the velocity is known or assumed, and the magnitude of the lift coefficient is to be calculated. Therefore, an analysis of the experimental data was undertaken to develop an equation that would predict the terminal velocity of the sphere in terms of the same variables that predicted the lift coefficient. The simultaneous solution of these prediction equations eliminated the angle term and presented the lift coefficient in terms of the velocity, viscosity, and diameter ratio.

Alternate Prediction Equation for the Lift Coefficient

An alternate method was used to develop the equation predicting the lift coefficient in order to simplify the form of the final equation. It was assumed that the lines plotted in Figures 7 - 9 are approximately parallel, since the magnitude of the standard errors of the slopes listed in Table 4 are quite large. Therefore, Equations 11 and 12 were

combined by addition to form a function $\pi_1 = f_4(\pi_2, \pi_3, \bar{\pi}_4)$, namely,

$$\pi_1 = 0.7663\ \pi_2 + 5.539 \times 10^{-7}\ \pi_3 - 0.0260 \qquad (25)$$

Equations 17 and 25 were also combined by addition. The alternate prediction equation, expressing π_1 as a function of the independent variables, is

$$\pi_1 = 0.7663\ \pi_2 + 5.539 \times 10^{-7}\ \pi_3 + 5.362 \times 10^{-4}\ e^{12.33\pi_4} - 0.0315 \qquad (26)$$

Terminal Velocity Prediction Equation

The expression relating the terminal velocity to the independent variables is

$$v = \phi_3 \left[d,\ D,\ \theta,\ \mu,\ \rho_f,\ \rho_s,\ g \right] .$$

Hence, in dimensionless form,

$$\frac{v^2}{gd} = \phi_4 \left[\sin\theta,\ \frac{\mu^2}{\rho_s^2\, gd^3},\ \frac{d}{D},\ \frac{\rho_s}{\rho_f} \right]$$

The term v^2/gd is designated as π_6, and the remaining ratios retain the symbols previously assigned.

Figure 16 represents the variation of π_6 with π_2

Figure 16. Variation of π_6 with π_2 while $\bar{\pi}_4 = 0.190$

Figure 17. Variation of π_6 with π_3 while $\bar{\pi}_4 = 0.190$

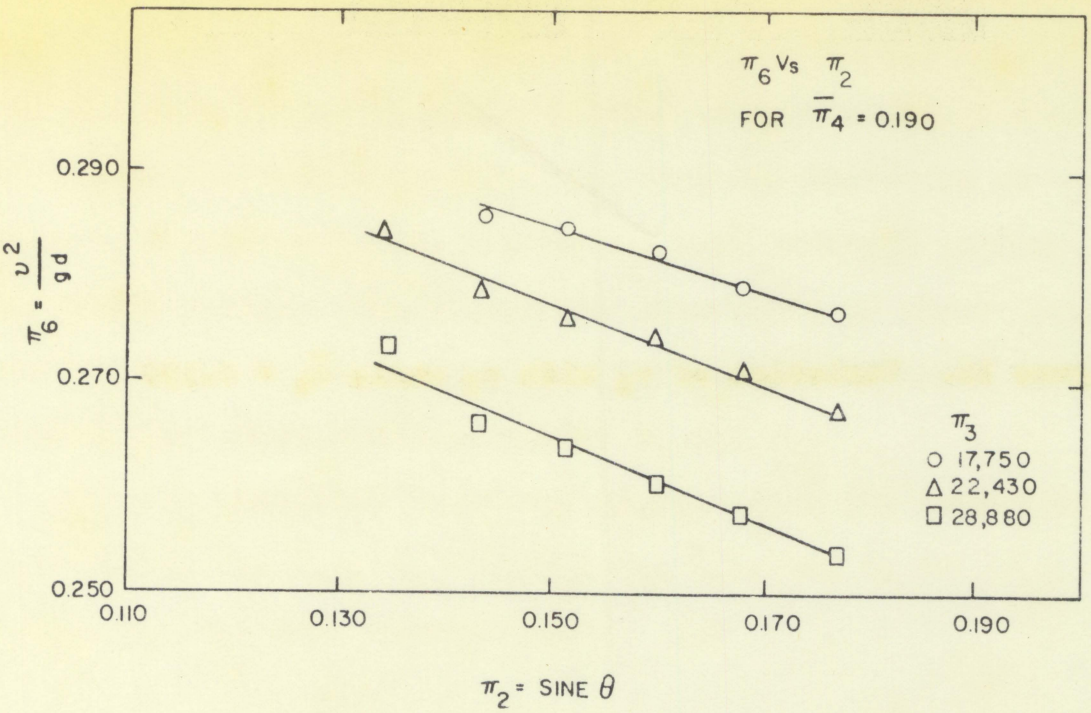
π_6 Vs π_2
FOR $\overline{\pi}_4$ = 0.190
$\pi_6 = \frac{v^2}{gd}$
0.290
0.270
0.250
0.110
0.130
0.150
0.170
0.190
π_3
○ 17,750
△ 22,430
□ 28,880
π_2 = SINE θ

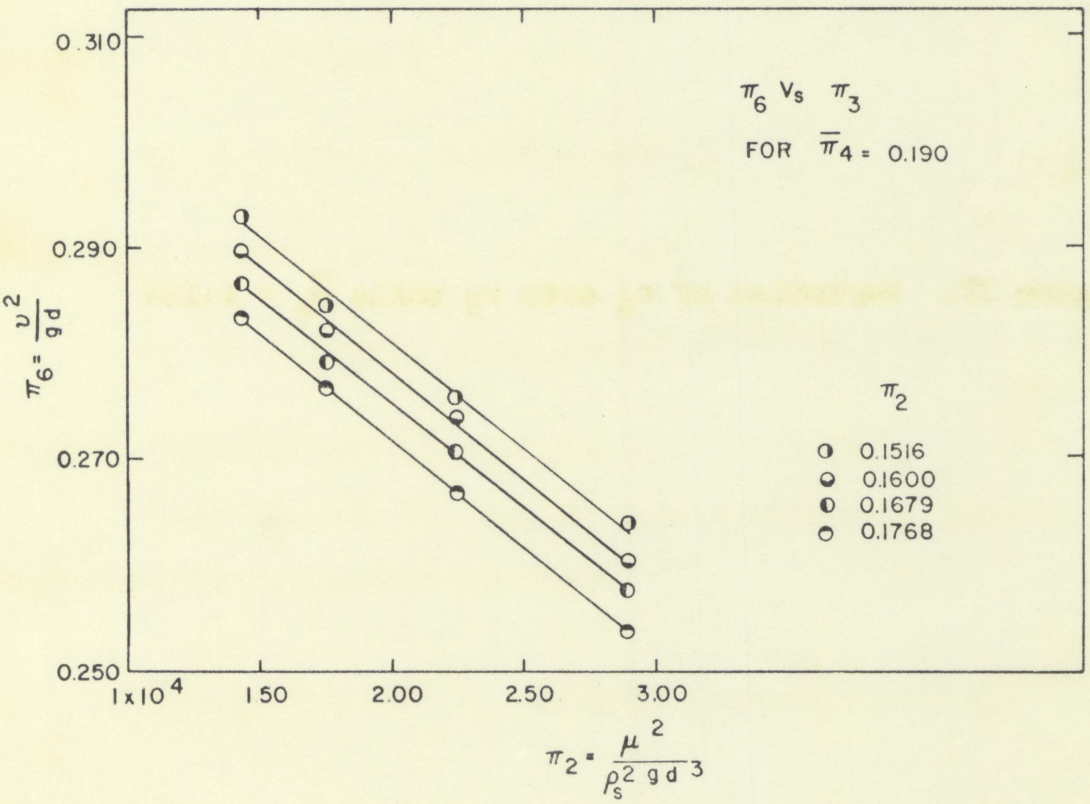
π_6 Vs π_3
FOR $\overline{\pi}_4$ = 0.190
$\pi_6 = \frac{v^2}{gd}$
0.310
0.290
0.270
0.250
1x10^4
1.50
2.00
2.50
3.00
π_2
0.1516
0.1600
0.1679
0.1768
$\pi_2 = \frac{\mu^2}{\rho_s^2 g d^3}$

while π_3 and π_4 are held constant. Slopes and intercepts of the data are listed in Table 8. The lines plotted in Figure 17 are approximately parallel and show the variation of π_6 with π_3 while $\bar{\pi}_4 = 0.190$, and π_2 was held constant at four different values. The slopes and intercepts of these lines are listed in Table 9. Figure 18 shows the variation of π_6 with π_4 for seven combinations of π_2 and π_3.

The component equations representing the functions $\pi_6 = f_5(\pi_2, \bar{\pi}_3, \bar{\pi}_4)$, $\pi_6 = f_6(\bar{\pi}_2, \pi_3, \bar{\pi}_4)$, and $\pi_6 = f_7(\bar{\pi}_2, \bar{\pi}_3, \pi_4)$ are, respectively

$$\pi_6 = 0.3258 - 0.2754\ \pi_2 \tag{27}$$

where $\bar{\pi}_3 = 17{,}750$ and $\bar{\pi}_4 = 0.190$,

$$\pi_6 = 0.3177 - 1.968 \times 10^{-6}\ \pi_3 \tag{28}$$

where $\bar{\pi}_2 = 0.1600$ and $\bar{\pi}_4 = 0.190$, and

$$\pi_6 = 0.3025 - 3.040 \times 10^{-3}\ e^{9.800\pi_4} \tag{29}$$

where $\bar{\pi}_2 = 0.1600$ and $\bar{\pi}_3 = 17{,}750$.

Equations 27, 28, and 29 were combined by addition to obtain the prediction equation

$$\pi_6 = 0.3803 - 1.968 \times 10^{-6}\ \pi_3 - 0.2754\ \pi_2 - 3.040 \times 10^{-3}\ e^{9.800\pi_4} \tag{30}$$

Figure 18. Variation of π_6 with π_4

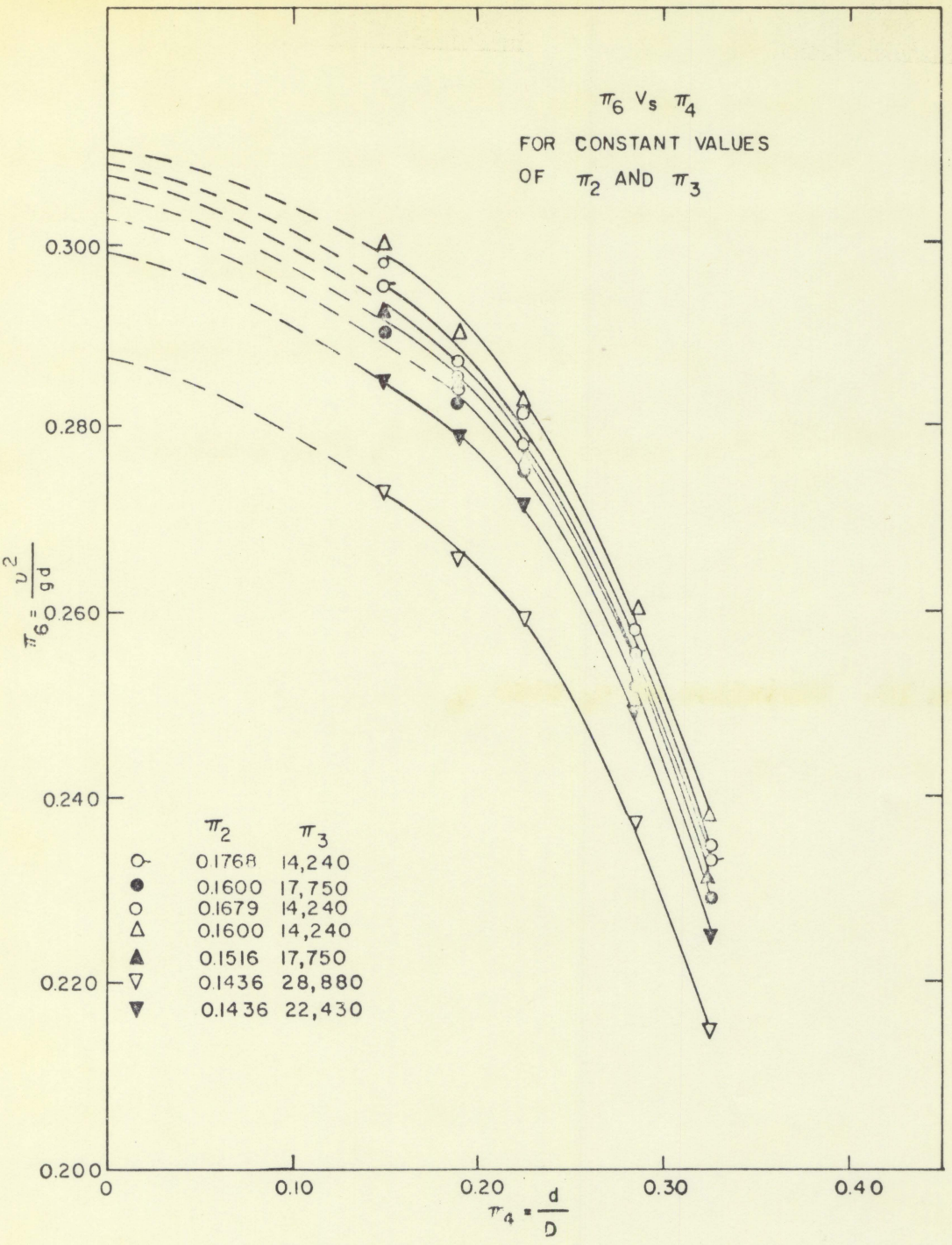
π_6 Vs π_4
FOR CONSTANT VALUES
OF π_2 AND π_3
$\pi_6 = \frac{v^2}{gd}$
0.300
0.280
0.260
0.240
0.220
0.200
0
0.10
0.20
0.30
0.40
$\pi_4 = \frac{d}{D}$
π_2 π_3
0.1768 14,240
0.1600 17,750
0.1679 14,240
0.1600 14,240
0.1516 17,750
0.1436 28,880
0.1436 22,430

Supplementary Lift Coefficient Equation

The supplementary lift coefficient equation, expressing π_1 as a function of the terminal velocity, viscosity, and diameter ratio, was obtained by eliminating π_2 in Equations 26 and 30. Hence,

$$\pi_1 = 1.0405 - 2.819\,\pi_6 - 4.993 \times 10^{-6}\,\pi_3 - 8.569 \times 10^{-3}\, e^{9.800\pi_4} + 5.362 \times 10^{-4}\, e^{12.33\pi_4} . \qquad (31)$$

SUMMARY AND CONCLUSIONS

The objective of this investigation was to study the influence of the pertinent variables on the lift coefficient of a single sphere moving in a circular tube. The investigation was accomplished with the aid of dimensional analysis. Eight variables, derived from the geometry, physical properties of the fluid and the phere, and the force system, were considered to be important. The group of variables was reduced to five dimensionless terms by using the Buckingham Pi theorem. One of the terms was assumed to be constant since its variation throughout the experiment was negligible. A general prediction equation was developed that related the lift coefficient to the variables investigated. In addition, a supplementary analysis was performed to eliminate the experimental term involving the inclination angle and introduce the velocity as an explicit variable.

Equation 24, which was developed to predict the lift coefficient in terms of the inclination angle, viscosity, and diameter ratio, is valid for the range of Pi terms investigated. The maximum percentage deviation from the experimental values was four percent. It must be noted that the range of variables was limited due to the requirement of non-rotational, rectilinear motion.

The equation derived to predict velocity in terms of

the angle, viscosity, and diameter ratio gives values that fall within five percent of the experimental values.

The supplementary lift coefficient equation (Equation 31) predicts the coefficient in terms of velocity, viscosity, and diameter ratio. Equations 24, 30, and 31 are valid for $\pi_5 = 1.14$ only, since the density ratio was assumed constant throughout the experiment, while π_6 ranged from 0.2153 to 0.2993, π_4 from 0.150 to 0.326, and π_3 from 14,240 to 28,880. Solutions to Equation 31 differ as much as 40 percent from the experiment when combinations of $\pi_6 \geq 0.2750$ and $\pi_3 \geq 22,430$ are used. Other values of the Pi terms result in agreement within five percent.

The following conclusions may be drawn from the results of the investigation:

1. In the range of particle Reynolds numbers investigated (approximately 200 to 550), viscosity is a pertinent variable and causes a decrease in the lift coefficient as it increases.
2. As the diameter ratio increases, the lift coefficient increases exponentially. As expected, the coefficient does not change rapidly as an infinite medium is approached, but it increases rapidly as the ratio becomes large and a Bernoulli effect becomes influential.
3. The presence of impurities in the form of fibrous particles greatly impairs the precision and accuracy of

an experiment of the type performed in this investigation.

4. Surface roughness, although not examined as a variable, was experimentally demonstrated to be an important factor.

5. The techniques employed to measure the lift coefficient over a limited range were satisfactory as shown by the degree of precision attained.

SUGGESTIONS FOR FURTHER INVESTIGATION

The tests in this investigation were conducted within a limited range of velocities. The range could be extended by examining the sphere as it rotates with a constant angular velocity and by different fluids.

It is recommended that the surface roughness of the sphere be examined as a variable. Tests should be conducted to determine the influence of the displacement of the sphere from the tube wall on the lift coefficient.

LITERATURE CITED

1. Jensen, V.G. Viscous flow round a sphere at low Reynolds numbers (less than 40). Royal Soc. of London Proc. Series A, 249: 349-366. 1959.

2. Stokes, G.G. On the effect of the internal friction of fluids on the motion of penduluns. Camb. Phil. Soc. Trans. 9, Part 2: 8-106. 1851.

3. Ladenburg, Rudolph. Über den Einfluss von Wänden auf die Bewegung einer Kugel in einer reibenden Flüssigkeit. Ann. der Physik. Series 4, 23: 447-458. 1907.

4. McNown, J.S., Lee, H.M., McPherson, M.B., and Engez, S.M. Influence of boundary proximity on the drag of spheres. Int'l Cong. for Appl. Mech., 7th, London, 1948. 2, Part 1: 17-29. 1948.

5. Young, Donald F. Lift and drag on spheres in circular tubes. Am. Soc. Civ. Eng. Proc. 86, Part 2: 47-57. 1960.

6. _____. The coring phenomenon in the flow of suspensions in vertical tubes. Am. Soc. Mech. Eng. Paper 60-HYD-12. Houston, Texas, Gas Turbine and Hydraulic Conference. 1960.

7. Rubinow, S.I. and Keller, Joseph B. Transverse force on a spinning sphere moving in a viscous fluid. J. of Fluid Mech. 11: 447-459. 1961.

8. Murphy, Glenn. Similitude in engineering. New York, N.Y., The Ronald Press Co. 1950.

9. Rose, Arthur and Rose, Elizabeth, ed. The condensed chemical dictionary. 5th ed. New York, N.Y., Reinhold Publishing Corp. 1956.

10. Worthing, Archie G. and Geffner, Joseph. Treatment of experimental data. New York, N.Y., John Wiley and Sons. 1955.

11. Topping, J. Errors of observation and their treatment. London, Inst. of Physics. 1955.

12. Davis, Dale S. Empirical equations and nomography. New York, N.Y., McGraw-Hill Book Co., Inc. 1943.

ACKNOWLEDGMENTS

The author is indebted to his major professor, Dr. Glenn Murphy, Head of the Department of Nuclear Engineering, for the support and guidance offered throughout the investigation and the preparation of the thesis. The suggestions and encouragement of Mr. Donald S. Sasscer, Assistant Professor of Nuclear Engineering, are gratefully acknowledged.

APPENDIX

Determination of the Standard Errors of the Measured Quantities

Velocity

Express the velocity as $v = x/t$, then, application of Equation 7 gives

$$\sigma_v^2 = \frac{1}{t^2}\sigma_x^2 + \frac{x^2}{t^4}\sigma_t^2$$

The standard errors of x and t may be estimated conservatively by assuming that they are the least measurements of the instruments used to determine them. The least measurements of the distance and time were, respectively, $\pm 2 \times 10^{-4}$ ft. and ± 0.017 sec. Thus, for the case $\bar{v}_2 = 0.1436$, $\bar{v}_3 = 17,750$, and $\bar{v}_4 = 0.190$,

$$\sigma_v = \pm 2.5 \times 10^{-5} \text{ ft./sec.}$$

Mass

The estimate of the error in the mass determination was

$$\sigma_M = \pm 6 \times 10^{-11} \text{ slug}$$

Sphere diameter

The standard error in determining the sphere diameter was calculated from the formula

$$\sigma^2 = \frac{\sum_{i=1}^{n} (\bar{d} - d)^2}{n(n-1)}$$

The value obtained was

$$\sigma_d = \pm 8 \times 10^{-6} \text{ ft.}$$

Sine θ

The inclination angle was obtained by measuring the legs of a right triangle. For $\bar{r}_2 = 0.1436$, the two legs were 2.90 ± 0.01 cm. and 18.90 ± 0.02 cm. The sine of the angle is $x/(x^2 + y^2)^{1/2}$ and

$$\sigma_{\sin\theta} = \pm 7.2 \times 10^{-3}$$

The individual contributions to the total error are:

$$\left(\frac{\partial C_L}{\partial H}\right)^2 \sigma_H^2 = 1.22 \times 10^{-9} \qquad \left(\frac{\partial C_L}{\partial V}\right)^2 \sigma_V^2 = 2.54 \times 10^{-14}$$

$$\left(\frac{\partial C_L}{\partial d}\right)^2 \sigma_d^2 = 1.75 \times 10^{-6} \qquad \left(\frac{\partial C_L}{\partial \sin\theta}\right)^2 \sigma_{\sin\theta}^2 = 3.41 \times 10^{-7}$$

The sum of these terms is

$$a^2_{C_L} = 2.09 \times 10^{-6}$$

or $$a_{C_L} = \pm 1.45 \times 10^{-3}$$

The controlling measurement is the determination of the sphere diameter. Except for the error in the angle measurement, the remaining terms may be neglected.

Table 4. Slopes and intercepts of r_1 versus r_2 data

r_4	r_3	Slope, b	Intercept, a
0.190	28,880	0.8811 ± 0.0106	-0.02769 ± 0.0017
	22,430	0.8233 ± 0.0090	-0.02259 ± 0.0014
	17,750	0.7663 ± 0.0124	-0.01569 ± 0.0020
	14,240	0.7964 ± 0.0186	-0.02276 ± 0.0031
0.226	28,880	0.8892 ± 0.0122	-0.02554 ± 0.0016
	22,430	0.8914 ± 0.0185	-0.02923 ± 0.0024
	17,750	0.8236 ± 0.0226	-0.02250 ± 0.0033
	14,240	0.792 ± 0.012	-0.0197 ± 0.007
0.285	28,880	0.931 ± 0.019	-0.0222 ± 0.003
	22,430	0.9439 ± 0.0169	-0.02826 ± 0.0026
	17,750	0.9007 ± 0.0145	-0.02497 ± 0.0007
	14,240	0.877 ± 0.012	-0.0240 ± 0.002

Table 5. Slopes and intercepts of π_1 versus π_3 data

π_4	π_2	Slope, b'	Intercept, a'
0.190	0.1768	7.503 x 10-7	0.1067
	0.1679	6.196 x 10-7	0.1020
	0.1600	6.029 x 10-7	0.0954
	0.1516	5.539 x 10-7	0.0900
0.226	0.1436	5.471 x 10-7	0.0862
	0.1345	5.434 x 10-7	0.0785
0.285	0.1679	8.660 x 10-7	0.1109
	0.1600	7.682 x 10-7	0.1055
	0.1436	6.057 x 10-7	0.0938

Table 6. Intercepts of π_1 versus π_4 curves

π_2	π_3	Intercept, E
0.1679	14,240	0.1040
0.1600	17,750	0.1014
0.1600	14,240	0.0984
0.1516	17,750	0.0940
0.1436	28,880	0.0935
0.1436	22,430	0.0896
0.1436	17,750	0.0870
0.1345	28,880	0.0851

Table 7. Comparison of experiment and Equation 24 values for the lift coefficient

π_2	π_3	$\pi_4 = 0.150$		$\pi_4 = 0.190$	
		Experiment	Equation	Experiment	Equation
0.1768	28,880			0.1282	0.1333
	22,430			0.1233	0.1278
	17,750			0.1198	0.1226
	14,240	0.1133	0.1148	0.1178	0.1170
0.1679	28,880			0.1200	0.1242
	22,430			0.1154	0.1193
	17,750			0.1128	0.1145
	14,240	0.1068	0.1072	0.1114	0.1094
0.1600	28,880			0.1131	0.1161
	22,430			0.1087	0.1118
	17,750	0.1034	0.1052	0.1063	0.1074
	14,240	0.1012	0.1005	0.1045	0.1027
0.1516	28,880			0.1058	0.1076
	22,430			0.1023	0.1037
	17,750	0.0974	0.0976	0.0999	0.0998
	14,240			0.0980	0.0955
0.1436	28,880	0.0968	0.0972	0.0994	0.0994
	22,430	0.0931	0.0938	0.0959	0.0960
	17,750	0.0909	0.0904	0.0943	0.0926
0.1345	28,880	0.0895	0.0879	0.0905	0.0901
	22,430			0.0882	0.0873

Table 7 (Continued)

π_2	π_3	π_4 = 0.226		π_4 = 0.285		π_4 = 0.326	
		Experiment	Equation	Experiment	Equation	Experiment	Equation
0.1768	22,430			0.1303	0.1317		
	17,750			0.1262	0.1270		
	14,240	0.1130	0.1125	0.1232	0.1218	0.1354	0.1337
0.1600	22,430			0.1227	0.1242		
	17,750	0.1091	0.1105	0.1192	0.1198	0.1310	0.1317
	14,240	0.1072	0.1058	0.1164	0.1151	0.1273	0.1270
0.1516	22,430			0.1152	0.1161		
	17,750	0.1028	0.1029	0.1118	0.1122	0.1229	0.1241
0.1436	28,880	0.1020	0.1025	0.1114	0.1118	0.1229	0.1237
	22,430	0.0985	0.0991	0.1072	0.1085	0.1186	0.1203
	17,750	0.0959	0.0957	0.1047	0.1050	0.1158	0.1169
0.1345	28,880	0.0940	0.0932	0.1030	0.1025	0.1138	0.1144
	22,430	0.0910	0.0904				
	17,750	0.0879	0.0875	0.0962	0.0968		
0.1264	28,880	0.0872	0.0849	0.0957	0.0942		
	22,430	0.0832	0.0826				
	17,750			0.0887	0.0895		
0.1188	28,880	0.0800	0.0771				
	22,430	0.0768	0.0743				
	17,750			0.0820	0.0826		

Table 8. Slopes and intercepts of π_6 versus π_2 data, with π_4 = 0.190

π_3	Slope	Intercept
28,880	-0.4309	0.3298
22,430	-0.3791	0.3341
17,750	-0.2754	0.3258

Table 9. Slopes and intercepts of π_6 versus π_2 data, with π_4 = 0.190

π_2	Slope	Intercept
0.1768	-2.040×10^{-6}	0.3130
0.1679	-1.996×10^{-6}	0.3146
0.1600	-1.968×10^{-6}	0.3177
0.1516	-1.955×10^{-6}	0.3201

Table 10. Comparison of experimental and Equation 31 values for C_L

π_4	π_3	π_6	Experiment	Equation
0.150	28,880	0.2731	0.0968	0.0927
		.2766	.0895	.0828
	22,430	.2849	.0931	.0917
	17,750	.2903	.1034	.0998
		.2922	.0974	.0945
		.2964	.0909	.0826
	14,240	.2951	.1133	.1038
		.2975	.1068	.0970
		.2993	.1012	.0920
0.190	28,880	.2541	.1282	.1304
		.2578	.1200	.1200
		.2606	.1131	.1121
		.2640	.1058	.1025
		.2661	.0994	.0966
		.2736	.0905	.0755
	22,430	.2670	.1233	.1263
		.2709	.1154	.1153
		.2741	.1087	.1063
		.2759	.1023	.1012
		.2788	.0959	.0930
		.2839	.0882	.0786
	17,750	.2768	.1198	.1220
		.2792	.1128	.1153
		.2823	.1063	.1065
		.2846	.0999	.1000
		.2857	.0943	.0969
	14,240	.2839	.1178	.1195
		.2869	.1114	.1111
		.2897	.1045	.1032
		.2930	.0980	.0939
0.226	28,880	.2593	.1020	.0956
		.2636	.0940	.0835
		.2672	.0872	.0734
		.2735	.0800	.0556
	22,430	.2715	.0985	.0934
		.2751	.0910	.0833
		.2828	.0832	.0615
		.2881	.0786	.0466

Table 10 (Continued)

π_4	π_3	π_6	Experiment	Equation
0.226	17,750	0.2751	0.1091	0.1066
		.2767	.1028	.1021
		.2810	.0959	.0900
		.2869	.0879	.0733
	14,240	.2779	.1204	.1162
		.2814	.1130	.1064
		.2826	.1072	.1030
0.285	28,880	.2375	.1114	.1049
		.2407	.1030	.0959
		.2432	.0957	.0889
	22,430	.2399	.1303	.1304
		.2428	.1227	.1222
		.2451	.1152	.1157
		.2493	.1072	.1039
	17,750	.2496	.1262	.1264
		.2518	.1192	.1202
		.2544	.1118	.1129
		.2571	.1047	.1053
		.2622	.0962	.0909
		.2674	.0887	.0762
		.2718	.0820	.0628
	14,240	.2553	.1311	.1279
		.2578	.1232	.1208
		.2601	.1164	.1143
0.326	28,880	.2151	.1229	.1108
		.2176	.1138	.1038
	22,430	.2253	.1186	.1143
	17,750	.2290	.1310	.1272
		.2314	.1229	.1204
		.2325	.1158	.1173
	14,240	.2329	.1436	.1337
		.2347	.1354	.1286
		.2378	.1273	.1199